

# A component library framework for deriving kinetic mechanisms for multi-component fuel surrogates: application for jet fuel surrogates

Krithika Narayanaswamy<sup>a,\*</sup>, Heinz Pitsch<sup>b</sup>, Perrine Pepiot<sup>c</sup>

<sup>a</sup>Department of Mechanical Engineering, Indian Institute of Technology Madras, Chennai – 600036, India

<sup>b</sup>Department of Mechanical Engineering, RWTH, Aachen, Germany

<sup>c</sup>Sibley School of Mechanical and Aerospace Engineering, Cornell University, New York – 14853, USA

## Abstract

Surrogate fuels are often used in place of real fuels in computational combustion studies. However, many different choices of hydrocarbons to make up surrogate mixtures have been reported in the literature, particularly for jet fuels. To identify the best choice of surrogate components, the capabilities of different surrogate mixtures in emulating the combustion kinetic behavior of the real fuel must be examined. To allow extensive assessment of the combustion behavior of these surrogate mixtures against detailed experimental measurements for real fuels, accurate and compact kinetic models are most essential. To realize this goal, a flexible and evolutive *component library framework* is proposed here, which allows mixing and matching between surrogate components to obtain short chemical mechanisms with only the necessary kinetics for the desired surrogate mixtures. The idea is demonstrated using an extensively validated multi-component reaction mechanism developed in stages [Blanquart *et al.*, *Combust. Flame* (2009), Narayanaswamy *et al.*, *Combust. Flame* (2010, 2014, 2015)], thanks to its compact size and modular assembly. To display the applicability of the component library framework, (i) a jet fuel surrogate consisting of *n*-dodecane, methylcyclohexane, and *m*-xylene, whose kinetics are described in the multi-component chemical mechanism is defined, (ii) a chemical model for this surrogate mixture is derived from the multi-component chemical mechanism using the component library framework, and (iii) the predictive capabilities of this jet fuel surrogate and the associated chemical model are assessed extensively from low to high temperatures in well studied experimental configurations, such as shock tubes, premixed flames, and flow reactors.

**Keywords:** Chemical mechanism, kinetics, jet fuel, surrogates, *n*-dodecane, substituted aromatics, methylcyclohexane, define surrogates, component library framework

## 1. Introduction

Transportation fuels, including aviation fuels, represent the largest part of petroleum based fuel consumption. For most civilian and military aviation, kerosene type (Jet-A/Jet A-1/JP-8) jet fuels are used. These jet fuels adhere to the general physical property specifications [1], which include heating value, smoke point, luminosity factor, aromatic content, volatility, viscosity, freezing point, and thermal stability of the fuel, among the properties relevant to the quality of combustion. The important differences between these fuels are that: Jet-A and Jet A-1 have different freezing points ( $-40^{\circ}\text{C}$  for Jet-A and  $-47^{\circ}\text{C}$  for Jet A-1) [2], and JP-8 includes an additive package to Jet A-1 to satisfy military requirements. However, the JP-8 additives have been found to have negligible influence on the fuel reactivity, and the ignition delays of Jet-A and JP-8 fuels show no differences at low to high temperatures [3]. Like typical transportation fuels, jet fuels are mixtures of several hundreds of compounds belonging to

different hydrocarbon classes. Their composition is found to vary from one source to another [4, 5], and only average fuel properties are known at best.

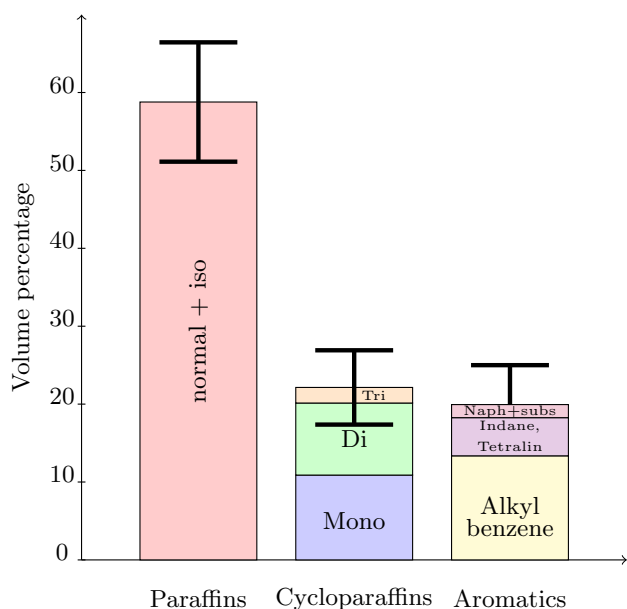
In computational studies, it is important to incorporate finite rate chemistry to understand the combustion characteristics of the real fuels, address the problem of combustion control, predict emissions, and optimize engine performance. However, the complexity of the real fuels makes it infeasible to simulate their combustion characteristics directly, requiring a simplified fuel representation to circumvent this difficulty. Typically, the real fuels are modeled using a representative *surrogate* mixture, *i.e.* a well-defined mixture comprised of a few components chosen to mimic the desired physical and chemical properties of the real fuel under consideration. These single or multi-component fuels are classified as *physical surrogates* if they have the same physical properties as the real fuel (density, viscosity, boiling and freezing temperatures, distillation curve, thermal conductivity, specific heat, etc.), or *chemical surrogates* if they have the same chemical properties (heat release rate and total heat release, fuel ignition, sooting tendencies, etc.) as the real fuel [6]. In this work, the interest is towards such a *chemical surrogate* for jet

\*Corresponding Author  
Email: krithika@iitm.ac.in

1 fuels, to represent the gas-phase chemical kinetic phenom-  
2 ena of the real fuel, in particular, heating value, major  
3 chemical classes, smoke point, density, average molecular  
4 weight, and reactivity.

### 6 1.1. Review of jet fuel surrogates and modeling approaches

7 Surrogates for real fuels are often chosen as mixtures of  
8 fuels representing the major hydrocarbon classes found in  
9 the real fuel. Chemical analysis [6–10] reveals the differ-  
10 ent hydrocarbon classes present in jet fuels, whose average  
11 composition is provided in Fig. 1. JP-8 fuel contains on  
12 average about 18% by volume of aromatics [10], with a  
13 maximum of 25%. The volume fraction of paraffins (nor-  
14 mal and branched) has a mean value of 58.78%, with a  
15 standard deviation of 7.66%, while the mono cycloparaffins  
16 have a mean value of 10.89%, with a standard deviation  
17 of 4.77% [7–9, 11].



41 Figure 1: Average composition of jet fuel from the the World Survey  
42 of Jet Fuels [7, 8] as summarized in Refs. [9, 11].

44 Several groups have proposed surrogates involving two,  
45 three, or more components for kerosene fuels and devel-  
46 oped kinetic models to describe their oxidation. An exten-  
47 sive review of the kinetic modeling efforts for jet fuels until  
48 2006 is available from Dagaut and Cathonnet [12]. Early  
49 studies modeled kerosene oxidation via quasi-global mod-  
50 els [13, 14] for the surrogate mixture. With the increase in  
51 computing capabilities, reduced and detailed mechanisms  
52 for the surrogates began to be proposed in place of global  
53 reaction models, for instance, in Refs. [15–20]. The kinetic  
54 models were validated for kerosene oxidation against the  
55 available ignition delay data at high temperatures [21, 22],  
56 species profile data in jet-stirred reactors [15, 17], and pre-  
57 mixed flames [23].

59 There is a large variation in composition of kerosene  
60 surrogates due to the wide variety of jet fuel applications [2].

The similarities between reactivities and product species  
profiles in *n*-decane and kerosene oxidation observed in  
experiments [15, 23] motivated many studies to include  
*n*-decane as the alkane class representative in their surro-  
gate mixtures, for instance, in Refs. [15–17, 19]. Normal  
dodecane was also used to represent the alkane class, since  
*n*-dodecane has physical properties similar to JP-7 and  
JP-8/Jet A [6], for instance, in Refs. [18–20]. In addition,  
small amounts of iso-octane or iso-cetane were included as  
surrogate components to represent the iso-alkanes in the  
real fuel, such as in Refs. [18, 20].

A number of studies compared various aromatic com-  
pounds in surrogates and concluded that alkyl-substituted  
aromatics were the best aromatic components [16, 24–  
29]. Xylenes, *n*-propylbenzene, *n*-butyl benzene, and  $\alpha$ -  
methyl naphthalene have all been considered as represen-  
tatives of the aromatic class, for instance, in Refs. [18–  
20, 30, 31]. In addition to paraffins and aromatics, Dagaut  
*et al.* [17, 32] observed that including a cycloalkane rep-  
resentative in the surrogate led to better agreement in aro-  
matics profiles between jet stirred reactor experimental re-  
sults and the model. Naphthenes such as methylcyclohex-  
ane, *n*-propylcyclohexane, and decalin have been used as  
cycloalkane representatives in several surrogate mixtures,  
for instance, in Refs. [17, 18, 20, 30, 33–35].

In most of the studies mentioned above, surrogates  
were defined such that average amount of the major chemi-  
cal classes in the jet fuel, given by 79% alkanes, 10%  
cycloalkanes, and 11% aromatics (by mole) [23, 36], was  
matched. In contrast, Violi *et al.* [18] proposed a strat-  
egy for surrogate formulation based on matching volatili-  
ty, sooting tendency, as well as combustion properties  
between the surrogate and the real fuel. Following the  
recommendations of Colket *et al.* [2], the surrogate defini-  
tion procedure for gas-phase combustion applications was  
subsequently refined in many later studies (for instance,  
Refs. [37–40]) to additionally reproduce *targets* such as  
hydrogen-to-carbon ratio, density, cetane number, thresh-  
old sooting index, and average molecular mass between the  
surrogate and the real fuel. A non-exhaustive summary of  
the recent surrogate formulation and kinetic modeling ef-  
forts is discussed in the following. Some of these studies  
have utilized a much wider experimental database [3, 39–  
52], which has become available in recent years, to validate  
their kinetic models for kerosene fuel oxidation.

Recently, Dooley *et al.* [39] proposed a surrogate for a  
specific Jet-A fuel (labelled POSF 4658) for gas-phase ap-  
plications, made up of *n*-decane, iso-octane, and toluene,  
to reproduce the aforementioned combustion targets, ex-  
cept that they considered derived cetane number over the  
conventional cetane number. The real fuel as well as the  
surrogate mixture were investigated experimentally in sev-  
eral configurations and found to show similar extents of  
chemical reactivities. They also proposed a kinetic model  
to represent their surrogate, compared against their ex-  
perimental data, and observed that the chemical reactivity  
of the surrogate is strongly dependent on the kinetics of

1 its *n*-alkane component. Since this surrogate had a lower  
2 molecular weight and TSI compared to the real fuel, Dooley  
3 *et al.* [40] proposed a second surrogate comprised of *n*-  
4 dodecane, iso-octane, *n*-propylbenzene, and 1, 3, 5-trimethyl  
5 benzene, which better matched the target Jet-A fuel. Their  
6 choice of surrogate components did not include every chemi-  
7 cal class present in the real fuel, but rather only those nec-  
8 essary to form intermediate species of markedly different  
9 potential for radical production and consumption.

10 This surrogate was studied experimentally, and found  
11 to exhibit essentially the same global combustion kinetic  
12 behavior as the real fuel. They also observed similar chemi-  
13 cal reactivities between the different surrogate fuels pro-  
14 posed in Refs. [39, 40] in flow reactors and shock tubes,  
15 which were traced back to equivalence in integrated pool of  
16 functionalities between the two surrogates. Based on these  
17 observations, Dooley *et al.* [40] conceptualized a *functional*  
18 *group based approach* to define surrogates with minimal  
19 complexity, knowing the average chemical structure and  
20 functionalities of the real fuel.

21 Malewicki *et al.* [52] developed a chemical model for  
22 this surrogate using the Dooley *et al.* [39] model as the  
23 base model and adding sub-models for *n*-propylbenzene  
24 and 1,3,5-trimethylbenzene, and predicted mole fractions  
25 of CO, CO<sub>2</sub>, C<sub>1</sub>-C<sub>3</sub> intermediate species and the decay of  
26 the surrogate fuel and oxygen in their shock tube experi-  
27 ments satisfactorily. Flow reactor simulations using their  
28 surrogate model captured the overall trends of the decay  
29 of O<sub>2</sub> and the formation of CO, CO<sub>2</sub>, and H<sub>2</sub>O. The com-  
30 puted ignition delays (above 750 K) predicted shock tube  
31 data within a factor of two.

32 Recently, Kim *et al.* [35] proposed a surrogate (UMI  
33 surrogates) containing *n*-dodecane, iso-cetane, toluene, and  
34 methylcyclohexane to represent various chemical and phys-  
35 ical properties relevant for spray development and ignition.  
36 They proposed a second surrogate containing decalin in-  
37 stead of methylcyclohexane, and found better match in  
38 physical properties between the surrogate and the real  
39 fuel. They modeled the surrogates using a detailed mech-  
40 anism [53] and predicted ignition delays at low to high  
41 temperatures within a factor of two.

## 42 1.2. Objectives of the present work

43 As noted from the discussion above, several surrogates  
44 have been proposed for jet fuels, and corresponding kin-  
45 etic models have also been developed. Existing chemical  
46 models for surrogate mixtures have considered several ex-  
47 perimental data sets for validation of component kinetics.  
48 However, a more comprehensive assessment of the individ-  
49 ual component kinetic description is necessary to predict  
50 the kinetic behavior of the surrogate mixtures with reli-  
51 ability. Further, to permit kinetic analysis, the kinetic  
52 schemes for surrogate mixtures must also be characterized  
53 by a compact size.

54 Our previous kinetic modeling efforts [54–57] have re-  
55 sulted in the development of a chemical mechanism for  
56

several hydrocarbons possessing these desirable character-  
istics. This reaction mechanism has been extensively vali-  
dated for many substituted aromatics [55], *n*-dodecane [56],  
and methylcyclohexane [57], and has the capability to de-  
scribe the oxidation of *n*-heptane and iso-octane, which  
are all important as components of transportation fuel  
surrogates. This multi-component chemical mechanism is  
also characterized by its compact size, consisting of 369  
species and 2691 reactions (counting forward and reverse  
reactions separately), and is hence amenable to chemical  
kinetic analysis.

Despite its compact size, an important feature of this  
kinetic model is its ability to predict oxidation at low  
through high temperatures for a number of molecular species.  
While conventional jet engines operate at high tempera-  
tures, an understanding of their ignition behavior at mod-  
erate and low temperatures is particularly important for  
controlling combustion in the context of using jet fuels in  
diesel [58–61] and HCCI type engines [2, 62]. Furthermore,  
the well-validated aromatic chemistry makes this reaction  
mechanism appropriate for assessing the formation of pol-  
lutants.

As evident from the literature on surrogate definition,  
there are several choices of hydrocarbons to make up sur-  
rogate mixtures for jet fuels. Note that while surrogate  
mixtures containing different components can be defined  
to possess the same global combustion properties, such as  
those described in section 1.1, there are likely to be differ-  
ences in their combustion dynamics that cannot be entirely  
prescribed by the global target properties. To reach con-  
sensus on the best choice of surrogate components, the ca-  
pabilities of different surrogate mixtures in emulating the  
combustion kinetic behavior of the real fuel must be eval-  
uated. To allow extensive assessment of the combustion  
behavior of these surrogate mixtures against detailed ex-  
perimental measurements for real fuels, accurate and com-  
pact kinetic models are essential.

As a first step towards this goal, we propose a flexible  
and evolutive *component library framework*, which allows  
mixing and matching between surrogate components to  
obtain short chemical mechanisms with only the necessary  
kinetics for the desired surrogate mixtures. The reaction  
mechanism described above, characterized by its compact  
size and modular assembly, lends itself into this frame-  
work naturally, and allows to be reorganized in the form  
of a parent mechanism containing sub-mechanisms of sev-  
eral component fuels. A chemical mechanism for a surro-  
gate mixture, the kinetics of whose individual components  
are described in this parent chemical mechanism, can be  
extracted from the library of component sub-mechanisms  
and validated extensively, thanks to its compact size.

The oxidation kinetics of several hydrocarbons relevant  
as transportation fuel surrogate components are described  
in the parent mechanism. Thus, short kinetic schemes  
for a large number of mixtures, which are potential sur-  
rogates for jet fuels, gasoline, diesel, and Fischer-Tropsch  
fuels can be extracted from the parent mechanism using

1 the component library approach and validated extensively.  
2 In this article, we demonstrate one specific example as an  
3 application of the component library approach by,

- 4 (a) defining a surrogate mixture to optimally represent the  
5 gas-phase combustion properties of an average jet fuel,  
6 consisting of molecules whose kinetics are described in  
7 the multi-component chemical mechanism described  
8 above [57],  
9
- 10 (b) deriving a chemical model for this surrogate mixture  
11 from the multi-component chemical mechanism [57]  
12 using the component library framework, and
- 13 (c) assessing the predictive capabilities of this jet fuel sur-  
14 surrogate and the chemical model extensively using data  
15 from well studied experimental configurations, such as  
16 shock tubes, premixed flames, and flow reactors.  
17

18 This article is organized as follows. In section 2, the  
19 development of the kinetic scheme referred above [54–57]  
20 is briefly described and reorganized into a component li-  
21 brary framework that allows to choose components whose  
22 kinetics need to be included in the chemical mechanism.  
23 Thereafter, in section 3, identifying *n*-dodecane, *m*-xylene,  
24 and methylcyclohexane as components of the jet fuel sur-  
25 surrogate, a constrained optimization approach is used to de-  
26 termine the surrogate composition that best represents the  
27 target properties of jet fuel. A chemical model to describe  
28 the oxidation of this surrogate is then derived from the  
29 multi-component chemical mechanism [57] using the com-  
30 ponent library approach. In section 4, the performance of  
31 the jet fuel surrogate and the kinetic scheme that describes  
32 its oxidation is assessed extensively against a much wider  
33 range of experimental data [3, 21, 23, 39–52] than previ-  
34 ously reported in the surrogate literature. The importance  
35 of the different surrogate fuel components towards global  
36 combustion characteristics are also discussed. The article  
37 is then concluded by highlighting the chief contributions.  
38

## 40 2. Reaction scheme for a multi-component fuel

41  
42 A compact chemical model valid for several fuels has  
43 been assembled in stages, starting with a well-validated  
44 base model for C<sub>0</sub>–C<sub>4</sub> chemistry [54] and adding to it  
45 sub-mechanisms for many hydrocarbons, which are rele-  
46 vant as components of transportation fuel surrogates [55–  
47 57]. Notably, this mechanism has the capability to de-  
48 scribe the oxidation of (a) several substituted aromatics,  
49 namely toluene (A<sub>1</sub>CH<sub>3</sub>), ethylbenzene (A<sub>1</sub>CH<sub>2</sub>CH<sub>3</sub>), styrene  
50 (A<sub>1</sub>C<sub>2</sub>H<sub>3</sub>), *m*-xylene (A<sub>1</sub>(CH<sub>3</sub>)<sub>2</sub>), and  $\alpha$ -methyl naphtha-  
51 lene (A<sub>2</sub>CH<sub>3</sub>), (b) *n*-heptane, (c) iso-octane, (d) *n*-dodecane,  
52 (e) methylcyclohexane, as well as soot precursor chemistry.  
53

54 The rate constants used for oxidation reactions of the  
55 aromatic species are obtained from the literature (exper-  
56 imental data and theoretical calculations) or are derived  
57 from those of the lower aromatics or the corresponding  
58 alkane species as described in Narayanaswamy *et al.* [55].  
59 The cyclopentadiene, naphthalene, and polycyclic aromatic  
60

(PAHs) chemistry are based on existing kinetic schemes as  
described in Blanquart *et al.* [54]. The sub-mechanisms for  
*n*-heptane, iso-octane, *n*-dodecane, and methylcyclohex-  
ane are incorporated by combining skeletal mechanisms  
for these hydrocarbons derived from appropriate detailed  
mechanisms [63–66] using model reduction techniques [67,  
68].

The merging of mechanisms is achieved using an in-  
teractive tool [38] that automatically identifies common  
species and reactions from different mechanisms and in-  
compatibilities between kinetic data sets, which are then  
resolved. Further, duplicate reaction pathways in the com-  
bined model coming from the incremental reaction scheme  
are identified and removed appropriately.

Note that combining different mechanisms has the risk  
of introducing truncated paths or involuntarily duplicat-  
ing reaction pathways, which has been best circumvented  
here by combining short skeletal reaction schemes. In  
fact, detailed models even for single components are of-  
ten of a large size, and therefore, combining these de-  
tailed mechanisms to create a multi-component mecha-  
nism of a size amenable to kinetic analysis would be nearly  
impossible. Combining skeletal mechanisms also ensures  
that only the kinetics essential to describe the oxidation  
pathways of desired hydrocarbons are introduced into the  
multi-component reaction mechanism, thereby resulting in  
a reasonably sized model.

Several revisions are incorporated to the reaction rate  
constants in the different sub-mechanisms based on recent  
experimental and theoretical rate calculations to improve  
the kinetic description as elaborated in Refs. [54–57]. The  
resulting chemical mechanism has been analyzed and val-  
idated comprehensively using available experimental data  
thanks to its reasonably compact size (369 species and  
2691 reactions counting forward and reverse reactions sep-  
arately). The validation test cases considered include 0D  
and 1D configurations, such as (i) ignition delays in shock  
tubes and rapid compression machines, (ii) burning speeds  
in laminar premixed flames, (iii) time history of species  
and radicals in shock tubes and flow reactors, and (iv)  
stable species and radical profiles in premixed flames. The  
validation tests for different fuels are shown in the main  
article corresponding to each component [54–57] and in  
the Supplementary materials of Ref. [57].

### *Component library approach*

As mentioned in section 1.2, to comprehensively ex-  
amine the capabilities of different surrogate mixtures to-  
wards reproducing the combustion kinetic behavior of the  
real fuel, short and accurate chemical kinetic models for  
these surrogate mixtures are essential. Note that having  
a compact size for the chemical model is important, be-  
cause a model with a reasonably small number of species  
(say <500) permits certain calculations, such as calcula-  
tion of laminar flame speeds, detailed species profiles in  
flames, sensitivity analysis, and integration in CFD sim-  
ulations (for example, using tabulation methods), which

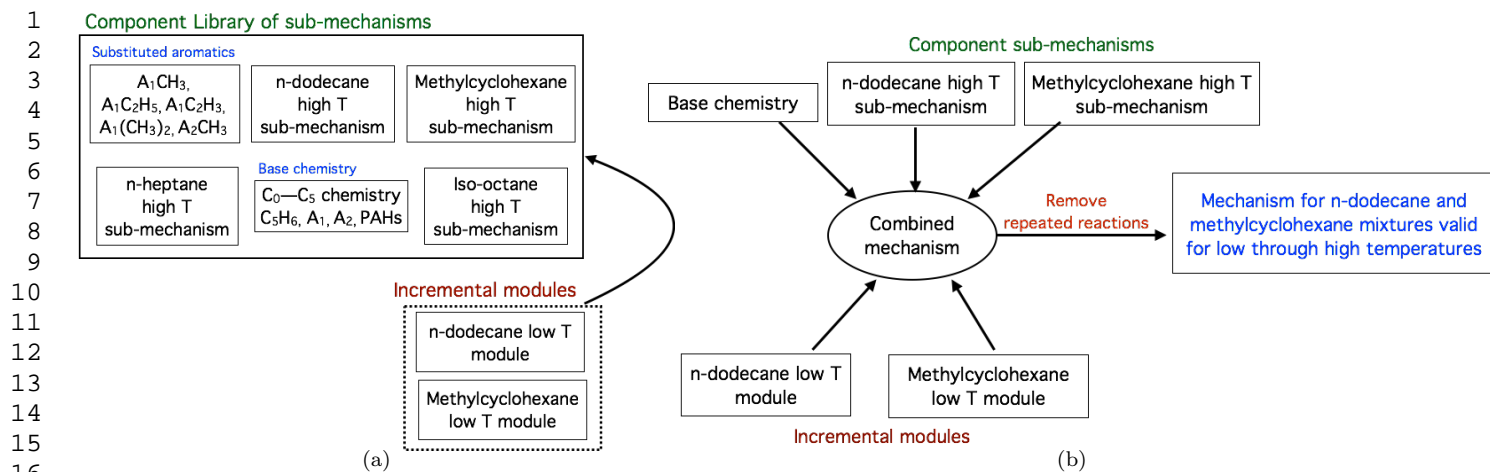


Figure 2: Left: Chemical model developed in Refs. [54–57] reorganized into a component library framework; Right: Assembling a chemical mechanism for *n*-dodecane and methylcyclohexane, valid from low to high temperatures, using the mix-and-match component library approach.

are difficult to do with larger reaction mechanisms. In this sub-section, we illustrate a flexible *component library framework*, which allows to mix and match between fuel components and obtain short chemical mechanisms with only the necessary kinetics for desired surrogate mixtures, using the multi-component chemical mechanism described above as an example.

This chemical mechanism is first rearranged into a parent mechanism, consisting of modules organized in the form of a *library of component sub-mechanisms*, namely those of high temperature oxidation of *n*-heptane, iso-octane, substituted aromatics, *n*-dodecane, and methylcyclohexane, with an underlying base chemistry for  $C_0$ – $C_5$  hydrocarbons, benzene, and PAH chemistry. The low temperature oxidation pathways of *n*-dodecane and methylcyclohexane are considered as incremental modules to this component library. This is pictorially represented in Fig. 2(a).

Having arrived at such a modular framework, short and accurate chemical mechanisms for desired single or multi-component fuels, whose kinetics are described in the parent mechanism, are obtained by combining relevant sub-mechanisms and incremental modules with the base chemistry. For instance, a kinetic scheme valid for low to high temperature oxidation of *n*-dodecane and methylcyclohexane is assembled by combining (i) base chemistry, (ii) high temperature sub-mechanisms for *n*-dodecane and methylcyclohexane, and (iii) incremental low temperature oxidation modules for *n*-dodecane and methylcyclohexane (see Fig. 2(b)). The duplicate reactions occurring in this combined mechanism are removed as a part of the post-processing step.

A perl script to generate kinetic models by picking desired sub-mechanisms and incremental modules from the multi-component mechanism described above [57] is available online [69] and in the Supplementary materials. Validation tests for selected multi-component mechanisms are also provided there.

Note that this modular component library based re-arrangement of the mechanism is readily feasible because direct cross-reactions between fuel-specific molecules (*i.e.* heavy molecular weight fuel radicals and intermediates) are not important for the kinetics in this reaction scheme. Rather, two different large hydrocarbon molecules interact during combustion only at the level of small radicals and decomposition products. The multi-component chemical kinetic scheme [57] also easily lends into being re-organized in this fashion owing to its compact size and development in stages. This component library idea can, in principle, be applied to chemical mechanisms that comply with these criteria, to obtain reaction schemes for a mixture of only a few components, whose kinetics are described in the parent mechanism.

This component library approach shares some similarities with Reaction Design’s Model Fuel Library (MFL) [70], which also has a library of sub-mechanisms for several hydrocarbons. In MFL, skeletal mechanisms for a desired multi-component fuel are obtained automatically using a combination of existing reduction techniques. However, in the present work, no model reduction is needed to extract the short multi-component mechanism, since the chemical mechanism [57] is already of a compact size and is in skeletal form. The open source perl script available in the Supplementary materials and online [69] is used to obtain the short mechanisms for the desired surrogate mixture.

Using this component library based re-arrangement of the multi-component kinetic scheme [57], reaction mechanisms for many hydrocarbon combinations can be extracted and used to assess potential surrogates for real fuels extensively. To give specific examples, at high temperatures, a mechanism for *n*-dodecane and iso-octane will be suitable to test mixtures of these components as Fischer-Tropsch surrogates [71]. The impact of substituting *n*-heptane in place of *n*-dodecane could also be examined, thus assessing the role of different alkanes in reproducing

1 combustion characteristics of the real fuel.

2 Similarly, a mechanism derived for low to high tem-  
3 perature oxidation of *n*-dodecane can be used to test this  
4 fuel as a single component diesel fuel surrogate, while a ki-  
5 netic scheme derived for *n*-dodecane in combination with  
6 *m*-xylene or  $\alpha$ -methyl-naphthalene could be used to under-  
7 stand the impact of aromatics in diesel surrogates; and  
8 a kinetic scheme derived for *n*-heptane, iso-octane, and  
9 toluene can be used to assess mixtures of these compo-  
10 nents as gasoline surrogates. Note that in deriving these  
11 kinetic schemes, only those kinetics necessary for the fuel  
12 components are included, thus resulting in smaller reac-  
13 tion mechanisms compared to the multi-component parent  
14 reaction scheme.

15 In this article, we demonstrate the applicability of this  
16 component library approach for jet fuel surrogates, by  
17 (i) deriving a short and accurate chemical model for a  
18 jet fuel surrogate from the parent multi-component mech-  
19 anism [57] and (ii) assessing the performance of the jet  
20 fuel surrogate and the chemical model extensively in well  
21 studied experimental configurations. As a first step, in the  
22 following section, a surrogate is defined to represent a jet  
23 fuel for gas-phase combustion applications.

24 The component library based on the multi-component  
25 chemical mechanism [57] will be expanded in the future  
26 to include the kinetics of additional hydrocarbons, which  
27 are relevant as transportation fuel surrogates, such as *n*-  
28 propylbenzene and *n*-propylcyclohexane. Further, the low  
29 temperature oxidation pathways of *n*-heptane and iso-octane  
30 will be added as incremental features, following a similar  
31 procedure as demonstrated for *n*-dodecane and methylcy-  
32 clohexane [56, 57] or by following the steps of Cai and  
33 Pitsch [72].

### 37 3. Jet fuel surrogate: Definition & Chemical ki- 38 netics

#### 39 3.1. Choice of jet fuel surrogate components

40 A natural procedure to select suitable components of a  
41 surrogate mixture for jet fuels is to identify one representa-  
42 tive hydrocarbon for each of the major hydrocarbon classes  
43 found in the real fuel, namely paraffins, cycloparaffins, and  
44 aromatics [6–9, 73] (shown in Fig. 1). This follows from  
45 the idea of choosing surrogate components from a palette  
46 of recommended species, as discussed in Refs. [2, 74, 75],  
47 for instance. This choice ensures that the different func-  
48 tional groups present in significant concentrations in the  
49 intermediate radical pool created during the combustion  
50 of the real fuel are adequately captured by the surrogate  
51 fuel. Establishing this correspondence in the intermediate  
52 radical pool is important to replicate the chemical kinetic  
53 behavior of the real fuel using the surrogate mixture [40].  
54 It is also essential to choose surrogate components that  
55 have been carefully studied [18], so that a comprehensive  
56 assessment of the surrogate kinetic model for the individ-  
57 ual component description is feasible, which is in itself

key to the performance of the multi-component surrogate  
model.

Based on molecules identified as relevant to jet fu-  
els [2], the components of the jet fuel surrogate for this  
work have been chosen as: (a) *n*-dodecane, to represent  
the paraffin class; (b) methylcyclohexane, to represent the  
naphthene class; and (c) *m*-xylene to represent the aro-  
matics. This choice is motivated by several observations.  
Longer chain alkanes, such as *n*-decane, *n*-dodecane, and  
*n*-tetradecane, are potential candidates to represent the  
paraffin class in jet fuel surrogates. Out of these normal  
alkanes, *n*-dodecane, which is used as a surrogate compo-  
nent in several studies, for instance, Refs. [18, 71], is a  
good compromise between a longer straight chain alkane,  
typical for transportation fuels, and a reasonable sized  
molecule [2]. Second, the aromatic component *m*-xylene  
possessing a higher tendency to soot compared to the other  
chosen components, helps the surrogate in reproducing the  
sooting characteristics of the jet fuel. Finally, methylcy-  
clohexane is the simplest substituted cyclic alkane that  
can be modeled reliably, and is therefore chosen as the  
cycloparaffin representative in the surrogate.

Dooley *et al.* [76] studied the importance of a cycloalkane  
functionality in the oxidation of a real jet fuel by experi-  
mentally studying the reactivities at low to high tempera-  
tures and laminar diffusion flame extinction limits of two  
surrogates: (a) a reference surrogate [39] and (b) a methyl-  
cyclohexane model fuel, consisting of 22.5% methylcyclo-  
hexane, having the same values for four selected combus-  
tion property targets, derived cetane number, hydro-  
gen/carbon ratio, molecular weight, and threshold soot-  
ing index. While no distinctive influence was observed  
on the low-temperature reactivity of the surrogate, the  
cycloalkane functionality was found to influence the hot-  
ignition transition by accelerating the global reactivity equiv-  
alent to an increase in reaction temperature of  $\sim 20$ – $30$  K  
at 800–900 K and 12.5 atm. These authors concluded that  
the cycloalkane class representative in the surrogate can  
perhaps be replaced with iso-alkane components.

However, the ring structure of these cyclic molecules  
allows specific pathways, for instance, opening of the cyclic  
ring, that are not possible in linear/branched alkanes/alkenes,  
which could potentially influence the reactivity of the real  
fuel. Further, cycloalkanes, for instance, methylcyclohex-  
ane, can directly form aromatic species (benzene and toluene)  
via dehydrogenation [57], while branched alkanes form aro-  
matics only through small hydrocarbons, such as acety-  
lene. In view of these unique kinetic features, a cycloalkane  
representative is included in the present jet fuel surrogate,  
as it could potentially influence the overall fuel reactivity  
and the aromatics formed from real fuel oxidation.

Note that although no iso-alkane is included as a sur-  
rogate component, this is partly compensated by includ-  
ing a cycloalkane representative in the surrogate mixture.  
Methylcyclohexane oxidation results in the formation of  
branched molecules such as radicals of iso-prene and *i*-C<sub>4</sub>H<sub>8</sub>  
that are characteristic of the intermediate radical pool of

1 iso-alkane oxidation. The importance of including a repre-  
2 sentative iso-alkane component in the jet fuel surrogate  
3 will be investigated in future.

### 4 3.2. Targets for combustion applications

5 Properties of typical transportation fuels that are cru-  
6 cial to design a surrogate for gas-phase combustion ap-  
7 plications include the fuel heating value, average carbon  
8 number, molecular weight, a measure of overall reactivity,  
9 and the sooting tendencies. These are described in de-  
10 tail here. The values of these target properties for a few  
11 transportation fuels are shown in Table 1.

12 *Heating value.* This target is crucial, since it determines  
13 the heat released and is hence important for the flame  
14 temperature. The lower heating value, which is the heat  
15 released when the combustion products are in gas phase is  
16 more relevant considering combustion in an engine. The  
17 heating value is correlated with a fundamental quantity,  
18 the H/C ratio, which is the ratio of the number of Hydro-  
19 gen atoms to the number of Carbon atoms in the fuel [38],  
20 as shown in Fig. 3(a). The higher the H/C ratio, the higher  
21 the energy released per unit mass of the fuel is.

22 The H/C ratio also correlates with the adiabatic tem-  
23 peratures for pure fuels [38] (see Fig. 3(b)), which using  
24 asymptotic arguments [82, 83] have been shown to be of  
25 leading order importance for laminar burning velocities.  
26 Figure 3(b) shows that an error in the H/C ratio of about  
27 0.1 leads to an error in the adiabatic flame temperature by  
28 about 8 K. Flame temperatures are also exceedingly im-  
29 portant for pollutant formation. For these reasons, match-  
30 ing the H/C ratio between the surrogate and the real fuel  
31 ensures the correct energy content, combustion tempera-  
32 ture, as well as flame speeds for the surrogate.

33 For instance, we consider six mixtures consisting of dif-  
34 ferent amounts of *n*-dodecane, methylcyclohexane, and *m*-  
35 xylene, such that their H/C ratios stay the same. It can  
36 be observed from Fig. 4(a) that the flame speeds of the  
37 pure components, especially for *m*-xylene, are different.  
38 However, the flame speeds for these mixtures, shown in  
39 Fig. 4(b), are the same to within 5% difference. Note that  
40 the mixtures considered (see caption of Fig. 4) have var-  
41 ied amounts of all the fuel components, ruling out any  
42 cancellation that might occur due to the flame speeds of  
43 *n*-dodecane and methylcyclohexane being similar. These  
44 different mixtures also result in similar integrated amounts  
45 of small radicals, as shown in the Supplementary materi-  
46 als, Fig. S1. The observed equivalence in the amounts of  
47 small radicals suggests that H/C ratio is also important  
48 for matching ignition delay times at high temperatures, as  
49 will be shown below.

50 The H/C ratio takes values between 1.9–1.95 for jet  
51 fuels and  $\sim 2.1$ – $2.2$  for Fischer-Tropsch fuels. Since this  
52 ratio varies depending on the hydrocarbon class (e.g.  $\sim 2$   
53 for alkanes, 1–1.4 for aromatics), this global quantity is  
54 also indicative of the diversity in the molecular structure  
55 in the real fuel.

*Molecular weight.* Fuel molecular diffusion properties are  
strongly related to the molecular weight [84]. Therefore,  
ensuring that the average molecular weight of the surro-  
gate fuel is similar to the real fuel is important to mimic  
the diffusive properties of the real fuel especially in laminar  
flames. If the real fuel and the surrogate have similar aver-  
age carbon numbers, then the equivalence ratios would be  
comparable. However, in turbulent flames, the effects of  
differences in magnitudes of molecular diffusion often van-  
ish. In these cases then, matching these properties might  
be unimportant [85].

*Reactivity.* Diesel and gasoline engines require accurate  
control of fuel reactivity, and this is globally indicated  
by cetane number (CN) and octane number (ON). Our  
previous investigations suggest that including the cetane  
number as a target in defining a surrogate for jet fuels  
is important for ignition delay predictions at intermed-  
iate temperatures, where the NTC regime of ignition pre-  
vails [71, 86].

Cetane number is experimentally determined by mea-  
suring the ignition delays of the fuel under consideration  
in a special diesel engine called a Cooperative Fuel Re-  
search (CFR) engine, and finding the specific mixture of  
iso-cetane and *n*-cetane which results in the same ignition  
delay. In this way, since the operating conditions under  
which cetane number is measured is that of a diesel en-  
gine, the cetane number is indicative of the ignition delays  
in the NTC regime of ignition. Higher cetane number cor-  
responds to faster ignition in the NTC region.

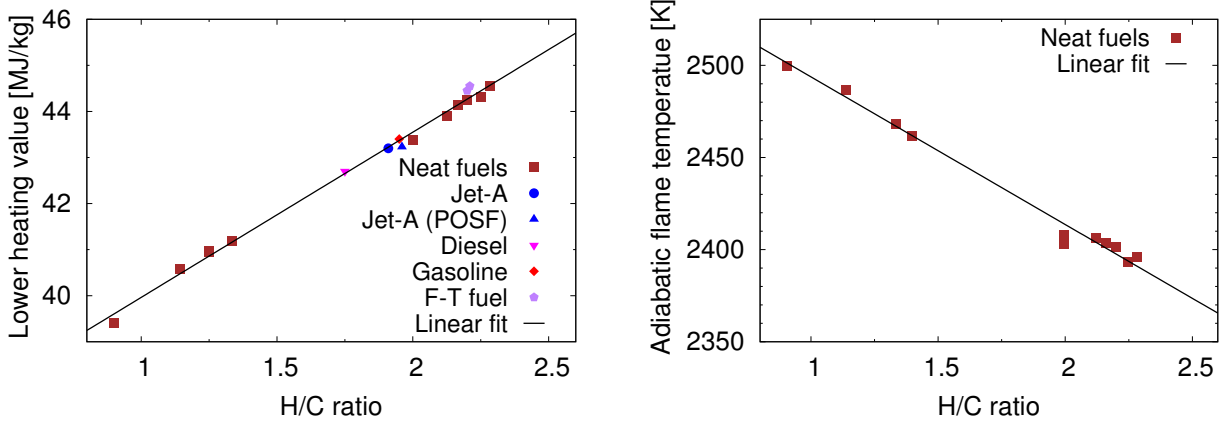
For instance, we consider three mixtures consisting of  
different amounts of *n*-dodecane, methylcyclohexane, and  
*m*-xylene, such that their cetane numbers stay the same. It  
can be observed from Fig. 5(a) that the pure components  
have vastly different ignition delay times at low through  
high temperatures. However, the ignition delays for their  
mixtures, which are shown in Fig. 5(b), while different at  
the high temperatures, all converge to similar values at  
moderate temperatures,  $700\text{ K} < T < 900\text{ K}$ .

Therefore, when considered as a target in the surrogate  
definition, the cetane number of the average jet fuel is  
representative of the autoignition quality of the fuel at  
intermediate temperatures. From the earlier discussion,  
note that H/C ratio is indicative of the small radical pool  
at high temperatures, which is important for ignition at  
these temperatures. In fact, the ignition delays computed  
using mixtures of *n*-dodecane, methylcyclohexane, and *m*-  
xylene, keeping the H/C ratio fixed yields similar ignition  
delays at high temperatures (maximum difference of 12%),  
as shown in Fig. 5(c). Thus, the cetane number and H/C  
ratio are both important targets for surrogate definition to  
reproduce the reactivity of the real fuel from intermediate  
to high temperatures.

*Sooting tendency.* The sooting tendency of a hydrocar-  
bon is experimentally determined by measuring the smoke  
height  $H$ , which is the largest flame height without smoke

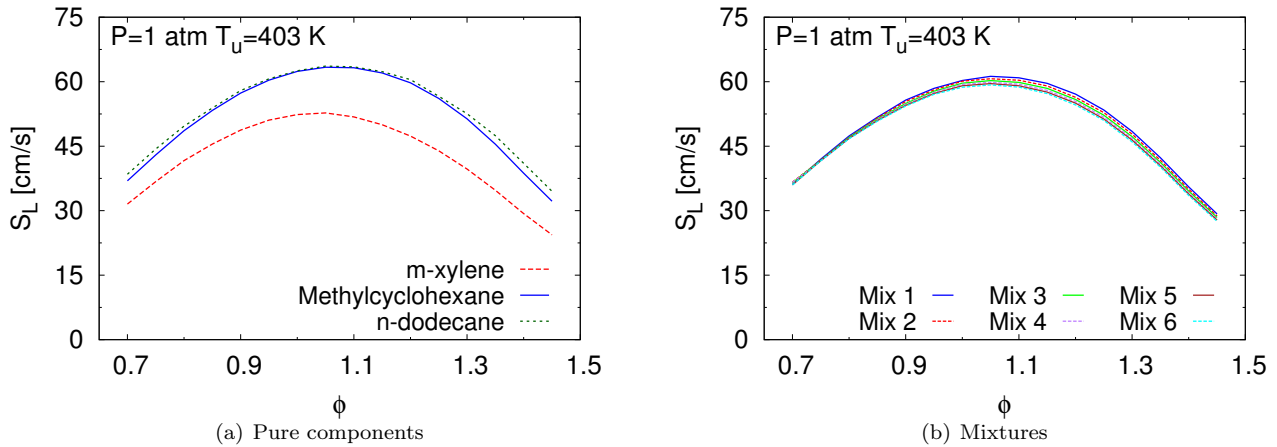
Parameters	Gasoline	Jet fuel	Diesel fuel	Fischer-Tropsch fuel
Lower HV (MJ/kg)	43.4	43.2	42.7	44.2
Carbon number range	4–12	8–16	9–23	–
Average formula	$C_{6.9}H_{13.5}$	$C_{11}H_{21}$	$C_{16}H_{28}$	–
Liquid density (kg/l)	0.735	0.775–0.840	0.850	0.736
Molecular weight (g/mol)	$\sim 96.3$	$\sim 153$	$\sim 220$	$163 \pm 15$
Threshold Sooting Index	–	14–26	–	–
Cetane Number	–	$\sim 42$	40–55	61

Table 1: Average properties of transportation fuels key to define surrogates for combustion applications. Data compiled from several sources [2, 5, 6, 73, 77–81].



(a) Correlation between lower heating value and H/C ratio (b) Correlation between adiabatic temperature and H/C ratio

Figure 3: Correlation between parameters describing the energy content and H/C ratio for neat fuels relevant as surrogate components and real petroleum-based transportation fuels.



(a) Pure components (b) Mixtures

Figure 4: Flame speeds at  $P = 1$  atm and  $T_u = 403$  K of (a) pure components and (b) mixtures of *n*-dodecane, methylcyclohexane, and *m*-xylene, with ratio  $H/C = 1.92$ ; Mixtures: *n*-dodecane/methylcyclohexane/*m*-xylene (mole %): Mix 1: 10%/76.5%/13.5%, Mix 2: 20%/62.4%/17.6%, Mix 3: 30%/48.4%/21.6%, Mix 4: 40%/34.3%/25.6%, Mix 5: 50%/20.3%/29.7%, Mix 6: 60%/6.2%/33.8%; Simulation results are obtained using the multi-component reaction scheme [57].

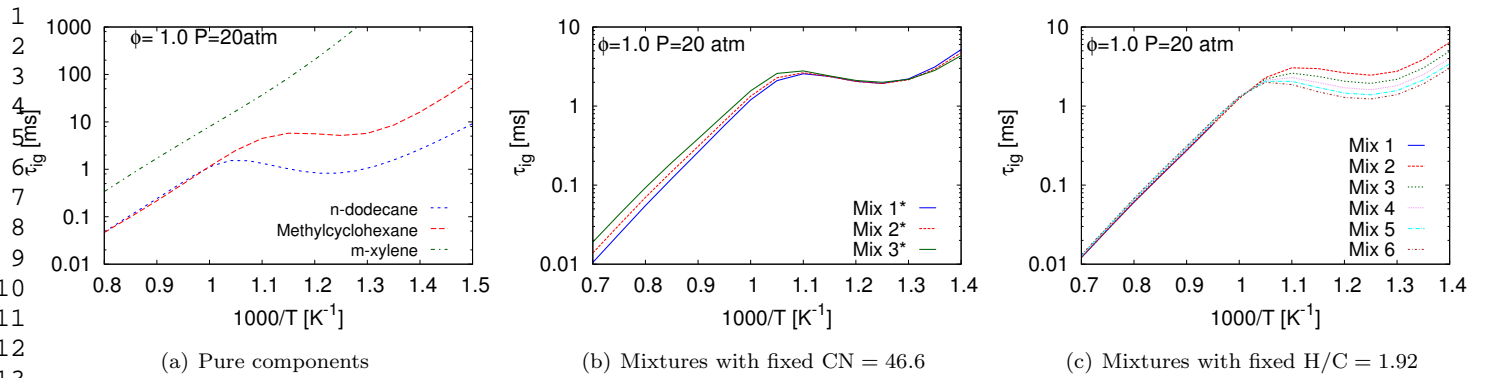


Figure 5: Ignition delays of (a) pure components, (b, c) mixtures of *n*-dodecane, methylcyclohexane, and *m*-xylene keeping targets fixed, predicted using the present reaction scheme; Mixtures: *n*-dodecane/methylcyclohexane/*m*-xylene (mole %): Mix 1\*: 29.2%/59.7%/11.1%, (ii) Mix 2\*: 31.1%/39.9%/29.0%, Mix 3\*: 33.1%/19.8%/47.1%; Mix 1–6: same as Fig. 4.

emission under laminar diffusion combustion. Smoke heights measured in a specific apparatus are converted into apparatus-independent *threshold sooting indices* (TSIs) using,

$$\text{TSI} = a \times \frac{\text{MW}}{\text{H}} + b,$$

where MW is the molecular weight of the hydrocarbon and  $a$  and  $b$  are apparatus-specific constants chosen so that  $\text{TSI}_{\text{ethane}} = 0$  and  $\text{TSI}_{\text{naphthalene}} = 100$  [87]. The threshold sooting index has been found to correlate well with actual particulate emissions [88]. Therefore, this serves as an important target for surrogate definition to capture the sooting ability of the real fuel. The determination of the TSI for a given fuel mixture is described in the next section.

### 3.3. Surrogate definition

The important properties that the surrogate must share with the real fuel were discussed in the previous section. However, note that not all surrogate mixtures can reproduce the target properties exactly. For instance, in defining their jet fuel surrogate, Dooley *et al.* [39] allowed precedence for H/C ratio over TSI, since no proportion of the selected components would satisfy the TSI and H/C ratio simultaneously. Therefore, given a choice of components to make up the surrogate, our goal is to determine an optimal component composition, so that the properties of the surrogate fuel best resemble the target real fuel properties.

In the present work, this objective is formulated as a *constrained optimization* problem, following the lines of Pepiot [38]. The composition of surrogate components are the optimization variables, and average real fuel target properties are the desired optimization targets. The most important targets are imposed through the introduction of constraints in the optimization problem.

In order to perform the optimization, quantitative structure/property relationships must be available, relating the target real fuel properties to the fuel structure of the individual surrogate components and their mole fractions. In

this work, mixture properties are determined by exploiting the fact that most of these target real fuel properties are indeed bulk properties; the multi-component surrogate fuel's properties are hence expressed as combinations of individual component properties, appropriately weighted by mole fractions or volume fractions.

The relationships for different combustion targets between the individual fuel component values and their mixtures are given in Table 2. Structural group analysis is used to determine threshold sooting index of the individual fuel components following Pepiot *et al.* [89]. This procedure follows that described by Yan *et al.* [90], based on the initial work of Benson [91].

A linear volume fraction weighted mixing rule is used to estimate the cetane number of mixtures from those of the neat components [92, 93]. Although this model can be less accurate [94, 95] because of the non-linear interactions between the fuel molecules, in the absence of a more accurate relationship that describes the interactions between the neat molecules chosen in the surrogate and their mixtures, the linear blending model is used here. Also, due to its simplicity, this model permits easy integration into the proposed constrained optimization approach. This linear blending rule has been found to be reasonably accurate in previous works [96, 97] and has been adopted in recent studies, for instance, Refs. [98–100].

In this work, the combustion properties of the real fuel that are desired to be reproduced by the surrogate fuel, namely, H/C ratio, number of carbons and hydrogens, cetane number, and threshold sooting index, are used as optimization targets. The optimal surrogate composition is determined by minimizing the sum of squares of the deviation of the target property values from the mixture values weighted appropriately. The function to be minimized is thus given by,

$$F(X_1, X_2, \dots, X_N) = \sum_{j=1}^{N^P} \omega_j \left( 1 - \frac{P_{j,mix}}{P_{j,target}} \right)^2, \quad (1)$$

where  $N^P$  refers to the number of optimization target

---

Mixture properties = function (Neat components)

---

$$n_{\text{mix}}^{\text{H}} = \sum_{i=1}^N X_i n_i^{\text{H}}$$

$$n_{\text{mix}}^{\text{C}} = \sum_{i=1}^N X_i n_i^{\text{C}}$$

$$\text{H/C}_{\text{mix}} = \frac{n_{\text{mix}}^{\text{H}}}{n_{\text{mix}}^{\text{C}}}$$

$$\text{CN}_{\text{mix}} = \sum_{i=1}^N V_i \text{CN}_i$$

$$\text{TSI}_{\text{mix}} = \sum_{i=1}^N X_i \text{TSI}_i$$


---

Table 2: Relationships for different combustion targets between the individual fuel component values and their mixtures:  $X$  – gas mole fraction,  $V$  – liquid volume fraction,  $n^{\text{H}}$  – number of hydrogen atoms,  $n^{\text{C}}$  – number of carbon atoms,  $\text{CN}$  – cetane number,  $\text{TSI}$  – threshold sooting index; Individual components are indicated with subscript  $i$  and mixture with subscript ‘mix’;  $N$  is the total number of components in the surrogate mixture.

properties,  $P_{j,\text{target}}$  refers to the desired target value of the property  $j$ , and  $P_{j,\text{mix}}$  refers to the mixture value of the property  $j$ , estimated using mixture rules prescribed above. Unequal weights ( $\omega_j$ ) could be assigned to these targets to bias one with respect to the other, nevertheless, these are treated equally in the present work. Although there are no constraints imposed in this case from the combustion properties, one constraint that must be satisfied is the normalization condition,

$$\sum_{i=1}^N X_i = 1. \quad (2)$$

The minimization of the objective function,  $F$  in equation (1), subject to this constraint is performed using the non-linear constrained optimization function, *fmincon*, in MATLAB [101].

This constrained optimization approach can in principle be employed to define a surrogate for any real fuel whose relevant target properties are known. Note that if the optimization targets are all replaced by constraints, this approach would be indistinguishable from the notion of defining a specific surrogate for a specific fuel, proposed by Dooley *et al.* [40]. Thus, the proposed method to define surrogates can be conceived as a generalized approach that allows to determine an optimal surrogate that represents real fuel target properties in the best manner, which is applicable even in those cases where no combination of the chosen surrogate components can replicate all the targets exactly.

The optimal component composition of the jet fuel surrogate that is obtained by solving the constrained optimization problem with  $n$ -dodecane, methylcyclohexane, and  $m$ -xylene as the surrogate fuel components is provided in Table 3, where the target properties used are also listed.

The aromatics contribution is primarily determined by the Threshold Sooting Index requirement for the surrogate. It is not necessary to match the real-fuel fraction of each of the representatives in the surrogate mixture, since it is primarily the intermediate radical pool generated by the oxidation of these hydrocarbons that dictates the chemical kinetic behavior of the mixture [40].

Table 3 shows that the proposed jet fuel surrogate agrees with the target real fuel properties in terms of the H/C ratio, cetane number, and sooting tendency. However, discrepancies can be observed for the average chemical formula and the fuel molecular weight comparing the real jet fuel and the proposed surrogate. Using a heavier cyclic alkane in place of methylcyclohexane in the surrogate mixture could help match these targets better. The following section will show that the proposed surrogate adequately describes the combustion characteristics of the real fuels in a large number of kinetically controlled configurations. This surrogate will be referred to as  $\mathcal{S}_o$ , to denote that the surrogate has been defined using a constrained optimization approach.

This optimization based surrogate definition approach shares several similarities with the approaches of Mueller *et al.* [100] and Ahmed *et al.* [102], although it was developed independently [38]. With a set of targets that included physical property targets, Mueller *et al.* [100] proposed surrogates for FACE diesel fuels, by minimizing a similar form of the objective function as in equation (1). Ahmed *et al.* [102] combined their regression modeling that uses MATLAB’s optimization tool [101] with physical and chemical kinetics simulations to propose surrogates for FACE gasoline fuels. In addition, both these studies employed an iterative procedure to find the weighting factors that would result in the best surrogate and verified that the surrogates mimic the real fuel properties experimentally.

Note that the combustion characteristics of the surrogate proposed in the present work has not been validated against those of the average jet fuel experimentally, unlike some of the earlier works [39, 40, 102]. Nevertheless, we expect  $\mathcal{S}_o$  to represent the combustion characteristics of an average jet fuel satisfactorily based on the observations of Dooley *et al.* [39, 40], that gas phase surrogates defined by matching their target properties (which are similar to those considered in this work) show a good degree of agreement with experiments. It could be suspected that in diffusion dominated configurations (especially laminar flows), the real fuel may not be well represented by surrogate  $\mathcal{S}_o$ , and discrepancies can surface due to the mismatch in molecular weight between the two, as discussed by Dooley *et al.* [40].

### 3.4. Kinetics of jet fuel surrogate

The oxidation of  $\mathcal{S}_o$  consisting of 30.3%  $n$ -dodecane, 21.2%  $m$ -xylene, and 48.5% methylcyclohexane, is described using a kinetic scheme derived from the multi-component

Target properties	Jet-A/JP-8 properties	Jet fuel Surrogate ( $\mathcal{S}_o$ )
H/C ratio	$1.91 \pm 0.05$ [5, 77]	1.92
Average formula	$C_{11}H_{21}$ [5, 77]	$C_{8.73}H_{16.79}$
Molecular weight (g/mol)	153	121.8
TSI	14–26 [10, 88]	14.03
Cetane Number	42–47 [80, 98]	46.6
Liquid density (kg/l)*	0.810 [5, 77]	0.772
Composition (% volume)*	11.2–31.44% <i>n</i> -Paraffins [2, 9] $\sim$ 35–40% Iso-paraffins [2] $\sim$ 2% Olefins [5] $10.89 \pm 4.77$ Naphthenes [9] $17.7 \pm 3.1\%$ Aromatics [5, 9] Sulfur (490 ppm) [5]	44.0% <i>n</i> -dodecane 39.4% methylcyclohexane 16.5% <i>m</i> -xylene
Composition (% mole fraction)*		30.3% <i>n</i> -dodecane 48.5% methylcyclohexane 21.2% <i>m</i> -xylene

Table 3: Jet fuel surrogate proposed using constrained optimization approach, referred to as  $\mathcal{S}_o$  in the article. \*The density and composition of the surrogate mixture are computed in the post-processing step. The range of values for compositions of different hydrocarbon classes present in typical jet fuels as compiled from several sources [2, 5, 9, 10, 77, 80, 88, 98] is indicated.

reaction mechanism discussed in section 2 [54–57], following the component library approach. The mechanism is obtained by choosing the high temperature sub-mechanisms for the surrogate fuel components, namely, *n*-dodecane, methylcyclohexane, and *m*-xylene (*i.e.* aromatics) from the parent reaction scheme. The incremental low temperature modules of *n*-dodecane and methylcyclohexane are also included, since the low temperature kinetics of the jet fuel surrogate is also of interest here. The absence of a low temperature module for *m*-xylene is due to the fact that this fuel does not exhibit low temperature reactivity [103]. A pictorial representation of the mechanism assembly can be drawn following Fig. 2(b) and is shown for reference in the Supplementary materials, Fig. S2.

The resulting  $\mathcal{S}_o$  mechanism contains 362 species and 2653 reactions. Note that the mechanism is characterized by a similar size as the parent reaction scheme (having 369 species and 2691 reactions), due to the inclusion of several fuels described in the parent mechanism as well as low temperature chemistry. The mechanism and the corresponding thermodynamic and transport properties are available in the Supplementary materials.

#### 4. Validation tests

The capabilities of the jet fuel surrogate proposed in Table 3 ( $\mathcal{S}_o$ ) are now evaluated by comparing simulations against a large experimental database. The validation tests focus on oxidation environments, while leaving out other configurations in which kinetics are strongly coupled with diffusion, such as counterflow diffusion flame experiments, as the focus of the present work is mainly on the kinetics aspect. The experimental data sets considered include (i) ignition delays spanning wide ranges of temperatures, pressures, and equivalence ratios (ii) major

species in shock tubes, (iii) concentration profiles of fuel, oxidizer, and major products, measured in a flow reactor at low to moderate temperatures, (iv) laminar flame speeds obtained at different pressures and unburnt temperatures, and (v) detailed species measurements in a rich premixed flame at atmospheric pressure. The list of the validation tests is summarized in Table 4.

The database for validation includes experiments performed with both JP-8 as well as Jet-A as fuels. Note that although the compositions of JP-8 and Jet-A fuels are different (owing to the special additives in JP-8), validating the proposed surrogate ( $\mathcal{S}_o$ ) with the data obtained for both fuels is still appropriate, because these fuels share similar global combustion characteristics. This is corroborated by experiments, which show that JP-8 and Jet-A fuels show no significant differences in (i) ignition delays measured in shock tubes [3, 41], (ii) flame speeds [48, 49], (iii) extinction and auto-ignition based on laminar non-premixed flows [34], and (iv) low temperature oxidation behavior in plug flow reactors [104].

Also, note that the Jet-A and JP-8 fuels studied in the experiments might have different values for the target properties (H/C ratio, sooting index, cetane number, etc.), which fall within the ranges listed in Table 3, while the  $\mathcal{S}_o$  surrogate is representative of an average jet fuel (see section 3.3). Nevertheless, comparing results obtained using  $\mathcal{S}_o$  as the fuel with experiments performed with different JP-8 and Jet-A fuels is very valuable here, since this provides a common base to leverage all available experimental data for JP-8 and Jet-A fuels, and thereby (i) evaluate the consistency between different experimental datasets, especially for ignition delays, and (ii) assess the ability of the surrogate and the proposed mechanism to represent the experimental measurements.

Further,  $\mathcal{S}_o$  mimics the H/C ratio and cetane num-

Ignition delays		Flow Reactor	Laminar flame speed	Species profiles	
Shock tube	Rapid Compression Machine			Shock tube	Burner-stabilized flame
Vasu <i>et al.</i> [41]			Ji <i>et al.</i> [48]		
Freeman and Lefebvre [21]			Hui <i>et al.</i> [49]		
Gokulakrishnan <i>et al.</i> [42]			Singh <i>et al.</i> [50]	Malewicki <i>et al.</i> [52]	Douté <i>et al.</i> [23]
Dean <i>et al.</i> [43]	Valco <i>et al.</i> [46]	Dooley <i>et al.</i> [39]	Kumar <i>et al.</i> [51]	Dooley <i>et al.</i> [40]	
Zhu <i>et al.</i> [44]	Dooley <i>et al.</i> [39]	Natelson <i>et al.</i> [47]	Dooley <i>et al.</i> [40]		
Wang and Oehlschlaeger [3]					
Zhukov <i>et al.</i> [45]					

Table 4: Validation cases for jet fuels considered in the present study.

ber of Jet-A POSF 4658 closely, which is the fuel studied in a number of experiments considered for validation here [3, 39, 40, 49, 52]. Therefore, the comparisons between the results obtained from  $\mathcal{S}_o$  and these experiments are indeed suited to be evaluated critically. Nonetheless, note that, for a particular sample of jet fuel, a *specific surrogate* could be proposed following the approach demonstrated by Dooley *et al.* [40] or equivalently, setting all optimization targets in our surrogate definition approach as constraints, which must then be validated in a comprehensive manner.

In the following simulations, shock tube experiments are modeled using a constant volume homogeneous reactor configuration. The same ignition criterion as in the experiments is used to compute the ignition delay times. Constant pressure simulations under adiabatic conditions are used to model the flow reactor experiments. Laminar flame speeds have been calculated in a manner similar to that described in our previous works [54–57]. All numerical calculations have been performed using the FlameMaster code (version 3.3.10, [105]).

#### 4.1. Ignition delays

Before discussing the ignition delays for the proposed jet fuel surrogate, a comparison between the ignition delays computed for the neat components and the experimental data for the real jet fuel (Jet-A and JP-8) from Vasu *et al.* [41] is shown in Fig. 6. Note that *m*-xylene does not exhibit low temperature reactivity, a behavior which is also supported by experiments [103].

At high temperatures ( $T > 1000$  K), ignition delays of the major components, *n*-dodecane and methylcyclohexane, are similar to those of the real fuel. At moderate temperatures ( $750 \text{ K} < T < 900 \text{ K}$ ), the ignition delays for methylcyclohexane are longer and those for *n*-dodecane are shorter than the real jet fuel ignition delays. Therefore, it is optimistic that a surrogate mainly comprised of these two fuels would be able to predict the experimental measurements adequately. This will be the object of investigation in this section.

To illustrate another example, a short chemical mechanism consisting of 174 species and 1893 reactions derived for *n*-heptane, iso-octane, and toluene mixtures, based on the component library approach, is used to compute these component ignition delays. The ignition delays of *n*-heptane, iso-octane, and toluene at high temperatures are more

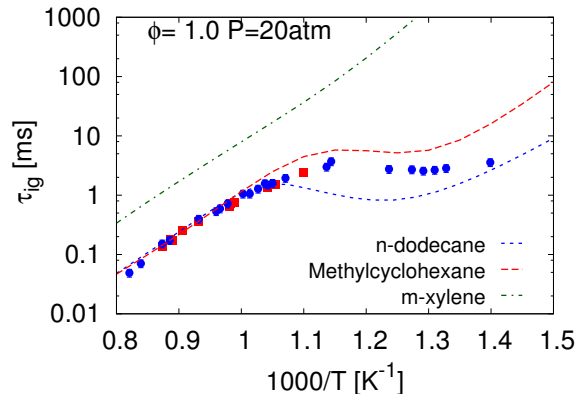


Figure 6: Comparing ignition delays of neat components of  $\mathcal{S}_o$  and Jet-A fuel; symbols - experimental data from Vasu *et al.* [41] for JP-8 (red) and Jet-A (blue) fuels; lines - results from simulations.

than twice longer compared to those of the real jet fuel (shown in Supplementary materials, Fig. S3). This suggests that no surrogate comprised of these hydrocarbons as components will be able to reproduce the ignition delay characteristics of real jet fuels satisfactorily.

##### 4.1.1. Fuel lean conditions

**4.1.1.1. Low pressures.** At atmospheric pressures and equivalence ratio of  $\phi = 0.5$ , Freeman and Lefebvre [21] and Gokulakrishnan *et al.* [42] measured ignition delays of Jet-A and JP-8 fuel, respectively, in a flow reactor. When compared to these data in Fig. 7(a), the simulations predict shorter ignition delays. However, when compared to the recent shock tube measurements of Zhu *et al.* [44] at  $P = 3$  atm in Fig. 7(b), it can be seen that the ignition delay predictions are almost within the quoted uncertainties in the measured data. In view of this, the reason for the differences in Fig. 7(a) could be speculated to be due to the inaccuracies introduced from modeling the flow reactor experiments of Gokulakrishnan *et al.* using an adiabatic homogenous constant volume reactor.

At similar lean conditions and higher pressures,  $P \sim 9$  atm, Dean *et al.* [43] measured ignition delays of Jet-A/air mixtures in a shock tube. Recently, Zhukov *et al.* [45] measured ignition delays at similar pressures using a heated shock tube at the same equivalence ratio using the same fuel sample as Dean *et al.* The comparison of the simulations with the data from Dean *et al.* shown in Fig. 7(c)

1 remains favorable, considering the scatter in their mea-  
 2 surements. The predicted ignition delays show less agree-  
 3 ment with the experimental data of Zhukov *et al.* Note  
 4 that Zhukov *et al.* introduced a correction to their mea-  
 5 surements ( $+7\ \mu\text{s}$ ) to account for the side wall rather than  
 6 the end wall ignition delay measurements. Therefore the  
 7 comparison at shorter ignition delays (such as  $10\text{--}20\ \mu\text{s}$  at  
 8  $T > 1250\ \text{K}$  in Fig. 7(c)) should be considered with caution.

9  
 10 *4.1.1.2. High pressures.* A comparison of computed igni-  
 11 tion delays with experimental measurements from Vasu *et*  
 12 *al.* [41] and Zhukov *et al.* [45] obtained in a shock tube  
 13 at  $P = 20\ \text{atm}$ , lean conditions ( $\phi = 0.5$ ), and high tem-  
 14 peratures, is shown in Fig. 8(a). Agreement between the  
 15 predictions and the experiments is good at these high tem-  
 16 peratures ( $T > \sim 1000\ \text{K}$ ). At  $T \sim 1050\ \text{K}$ , the simulations  
 17 agree well with the data from Vasu *et al.*, in comparison  
 18 to the data from Zhukov *et al.* Considering the discrep-  
 19 ancy between the data from Zhukov *et al.* [45] and Vasu  
 20 *et al.* [41] at  $T \sim 1100\ \text{K}$  at  $P = 20\ \text{atm}$ , it could be sur-  
 21 mised that the lowest temperature data point of Zhukov  
 22 *et al.* [45] in Fig. 7(c) could also be a under-prediction,  
 23 meaning a better agreement of the simulations at these  
 24 conditions.

25  
 26 Wang and Oehlschlaeger [3] measured ignition delays  
 27 of a Jet-A fuel (POSF 4658) fuel in a shock tube and in-  
 28 vestigated fuel/air mixtures of varying equivalence ratios  
 29 and at different pressures. Figure 8(b) shows that at lean  
 30 conditions of  $\phi = 0.5$ , the high temperature ignition de-  
 31 lays are predicted in good agreement with their experi-  
 32 mental measurements. This was also observed when compar-  
 33 ing against shock tube ignition delay data from Vasu  
 34 *et al.* [41] at similar experimental conditions in Fig. 8(a).  
 35 For leaner fuel/air mixtures,  $\phi = 0.25$ , in Fig. ??, the  
 36 simulated results agree best with the experiments at high  
 37 temperatures,  $T > 1100\ \text{K}$ . The predictions show deviations  
 38 compared to the experiments at lower temperatures (up to  
 39 a factor of 2),  $900\ \text{K} < T < 1100\ \text{K}$ . The simulations are in  
 40 better agreement at moderate and low temperatures at  
 41 equivalence ratio of  $\phi = 0.5$  in Fig. 8(b).

42  
 43 Considering Fig. 8(b), the simulations predict similar  
 44 slope of ignition delay time curve at moderate tempera-  
 45 tures where NTC regime of ignition persists,  $760\ \text{K} < T <$   
 46  $1000\ \text{K}$ , as well as at low temperatures,  $T < 760\ \text{K}$ . The  
 47 temperatures at which the ignition behavior transitions  
 48 from one regime to another (meaning the temperatures  
 49 at which the ignition delay time curve peaks or reaches a  
 50 minimum) also agree with the experimental data. How-  
 51 ever, the computations show an overall over-prediction of  
 52  $40\text{--}50\%$  compared to the measurements. Nevertheless, this  
 53 remains to be a favorable result for these moderate tem-  
 54 peratures.

#### 55 *4.1.2. Stoichiometric conditions*

56  
 57 *4.1.2.1. Low pressures.* The computed ignition delays are  
 58 compared with the measurements obtained by Zhu *et al.* [44]

in a shock tube at pressures  $P = 3$  and  $6\ \text{atm}$  and high tem-  
 peratures ( $T > 1100\ \text{K}$ ) in Fig. 9(a). The model predictions  
 show a very good agreement with their experimental data  
 set, falling within the uncertainties in the measurements.

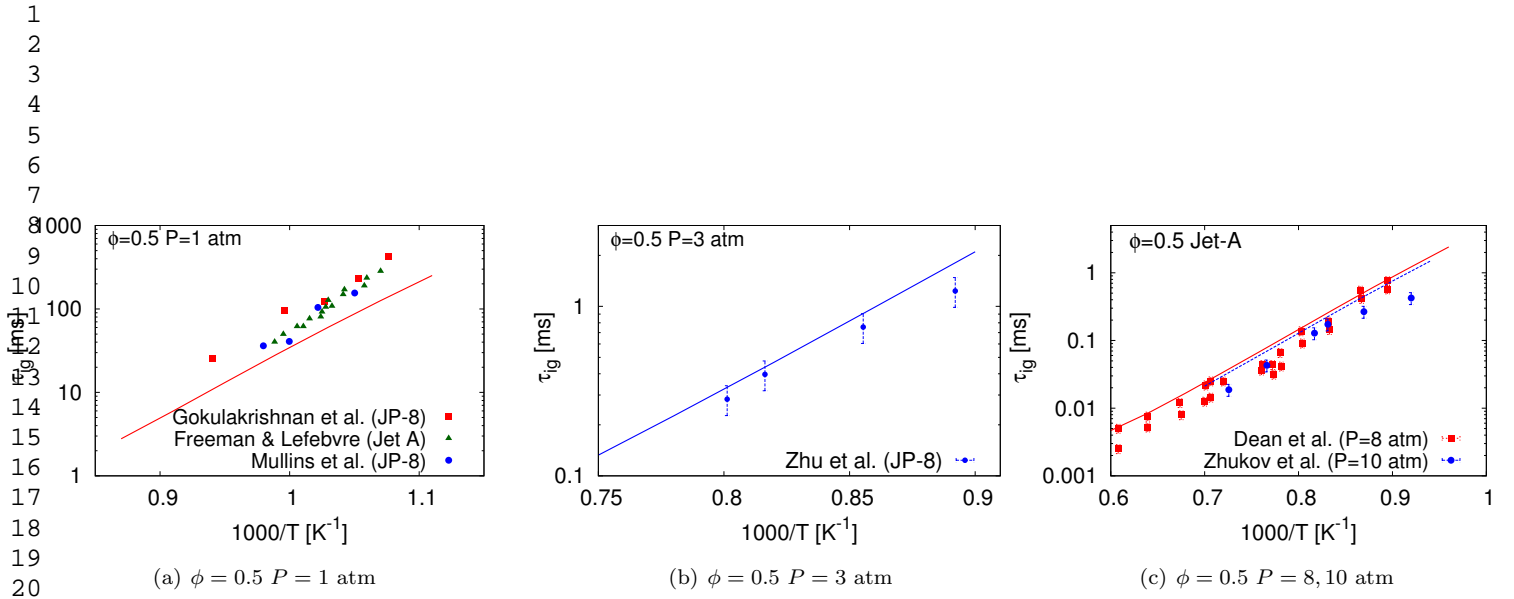
At pressures,  $P \sim 10\ \text{atm}$ , the simulated ignition delays  
 at  $\phi = 1.0$  are compared with the experimental data from  
 several groups [3, 43, 45] in Figs. 9(b)–9(d). The com-  
 puted results show an over-prediction compared to the ex-  
 perimental data from Dean *et al.* and Zhukov *et al.* at  
 high temperatures,  $T > 1000\ \text{K}$ , in Fig. 9(c), however, fall  
 with the experimental uncertainty of the data reported by  
 Wang and Oehlschlaeger at similar pressures (seen clearly  
 in Figs. 9(b) and 9(d)).

Wang and Oehlschlaeger [3] attribute the differences  
 between their data compared to the data from Dean *et al.*  
 to the chemiluminescence measurements made by Dean *et al.*  
 at the side wall locations. For highly exothermic reac-  
 tant mixtures, this can result in artificially shortened ob-  
 served ignition delay times [106] and appreciably affect the  
 short ignition delay times, such as at those temperatures  
 in Fig. 9(c). Also, note that the data of Dean *et al.* [43]  
 and Zhukov *et al.* [45] in Fig. 9(c) at  $P = 9$  and  $10\ \text{atm}$ , re-  
 spectively, lie below the data of Wang and Oehlschlaeger  
 at  $P = 11\ \text{atm}$  at temperatures  $1100 < T < 1400\ \text{K}$ , which  
 is counter-intuitive to the pressure dependence of ignition  
 delays at these temperatures. These arguments allow to  
 conclude that the present model predictions lie within the  
 experimental variability at the high temperatures.

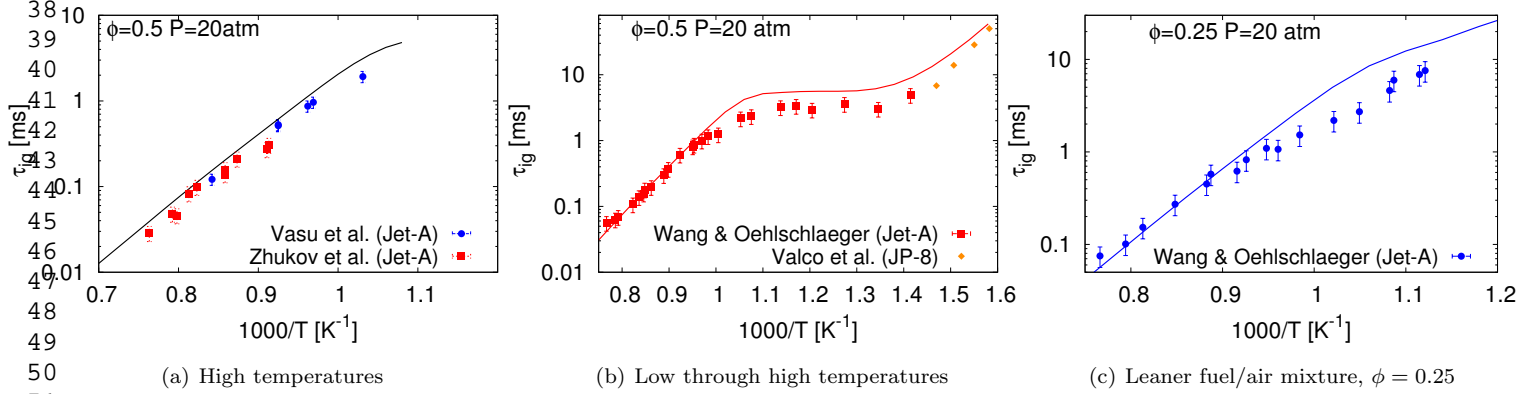
At the transition to the NTC ignition regime ( $850\ \text{K} <$   
 $T < 1000\ \text{K}$ ), the simulated results show an over-prediction  
 (up to  $60\%$ ) compared to the experimental data in Figs. 9(b)  
 and 9(d), however, fall within the uncertainty in the exper-  
 imental data at moderate temperatures ( $750\ \text{K} < T < 850\ \text{K}$ )  
 in Fig 9(d). At lower temperatures,  $700\ \text{K} < T < 750\ \text{K}$ , RCM  
 data from Valco *et al.* [46] seem to diverge from the data  
 of Wang and Oehlschlaeger [3]. Valco *et al.* attribute  
 this deviation to the physical compression stroke, where  
 at higher temperatures some pre-ignition chemistry could  
 be occurring [46].

59  
 60 *4.1.2.2. High pressures.* At  $P \sim 20\ \text{atm}$ , a comparison be-  
 61 tween the simulations and experimental data for different  
 62 jet fuels obtained in (a) shock tubes: Refs. [3, 41, 45],  
 63 and (b) Rapid Compression Machine: Refs. [39, 46] are  
 64 shown in Figs. 10(a) and 10(b). The computations show  
 65 a good agreement with the data at  $T > 1100\ \text{K}$ , following  
 the Wang and Oehlschlaeger data [3] closely, while show-  
 ing differences compared to those from Vasu *et al.* [41] and  
 Zhukov *et al.* [45] (see Fig. 10(a)).

The simulations show an excellent agreement with the  
 experimental data in Fig. 10(b) at  $T > 760\ \text{K}$ , with the slope  
 at the high temperatures and in the NTC ignition regime  
 well represented by the simulations. At lower tempera-  
 tures in Fig. 10(b), the simulations predict longer igni-  
 tion delays compared to the experiments of Wang and  
 Oehlschlaeger [3] and Valco *et al.* [46], while they agree  
 better with the experimental data from Dooley *et al.* [39].

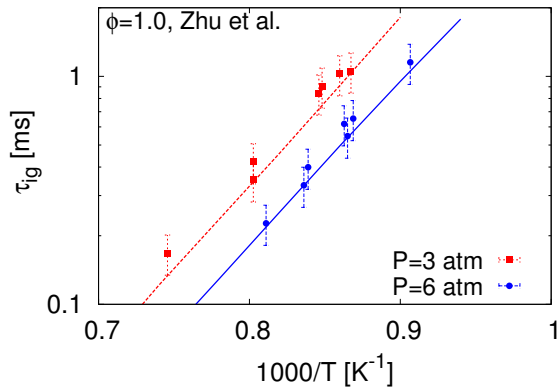


21  
22 Figure 7: Ignition delay times of JP-8/Jet-A fuels at lean fuel/air equivalence ratios: Symbols - experimental data from Freeman & Lefebvre [21], Gokulakrishnan *et al.* [42], Zhu *et al.* [44]; lines - results from simulations.

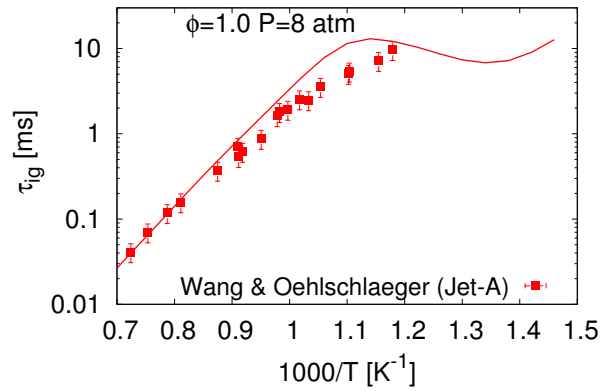


52 Figure 8: Ignition delay times of JP-8/Jet-A fuels at lean fuel/air equivalence ratios: Symbols - experimental data from Vasu *et al.* [41], Wang and Oehlschlaeger *et al.* [3], and Valco *et al.* [46]; lines - results from simulations.

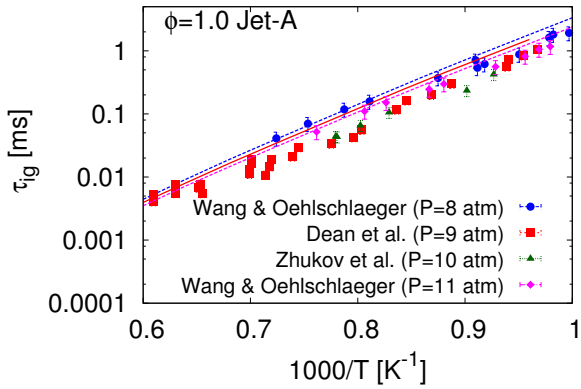
1  
2  
3  
4  
5  
6  
7  
8  
9  
10  
11  
12  
13  
14  
15  
16  
17  
18  
19  
20  
21  
22  
23  
24  
25  
26  
27  
28  
29  
30  
31  
32  
33  
34  
35  
36  
37  
38  
39  
40  
41  
42  
43  
44  
45  
46  
47  
48  
49  
50  
51  
52  
53  
54  
55  
56  
57  
58  
59  
60  
61  
62  
63  
64  
65



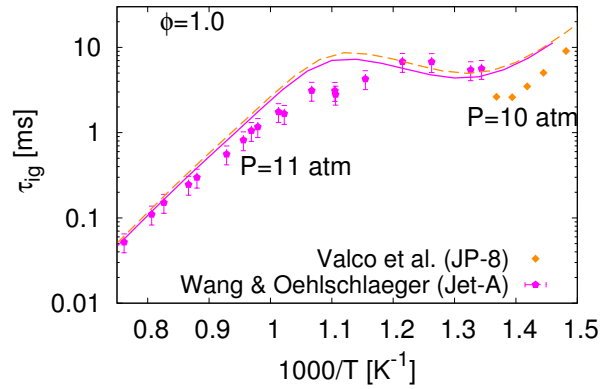
(a)  $\phi = 1$   $P = 3, 6$  atm



(b)  $\phi = 1$   $P = 8$  atm



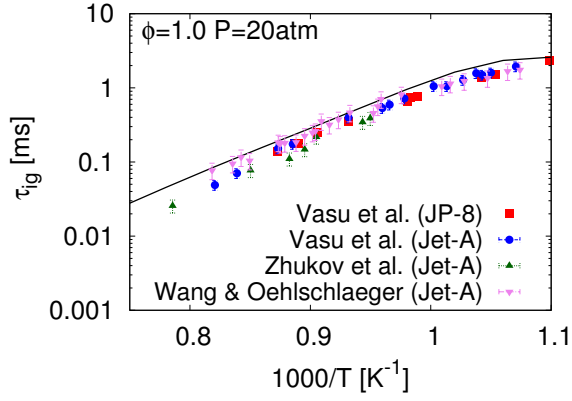
(c)  $\phi = 1$   $P = 8$  atm



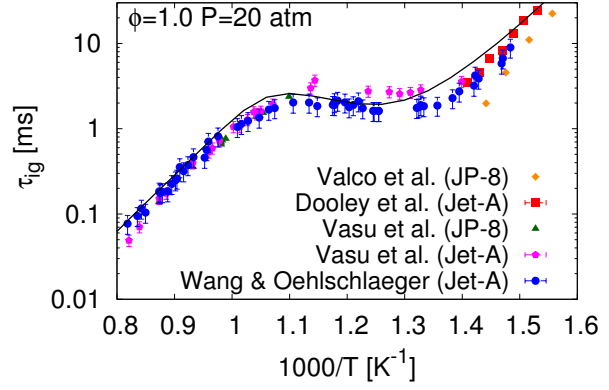
(d)  $\phi = 1$   $P = 11$  atm

Figure 9: Ignition delay times of JP-8/Jet-A fuels at stoichiometric fuel/air equivalence ratios: Symbols - experimental data from Wang and Oehlschlaeger *et al.* [3], Dean *et al.* [43], Zhu *et al.* [44]; lines - results from simulations.

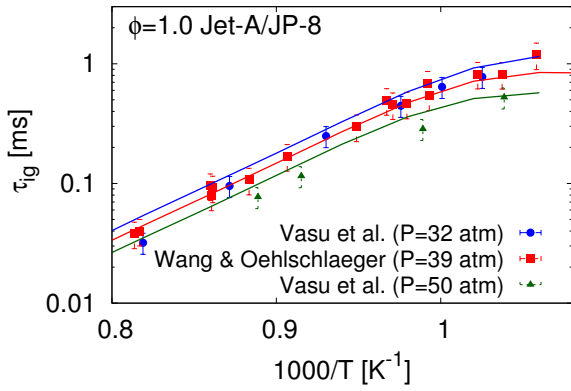
1  
2  
3  
4  
5  
6  
7  
8  
9  
10  
11  
12  
13  
14  
15  
16  
17  
18  
19  
20  
21  
22  
23  
24  
25  
26  
27  
28  
29  
30  
31  
32  
33  
34  
35  
36  
37  
38  
39  
40  
41  
42  
43  
44  
45  
46  
47  
48  
49  
50  
51  
52  
53  
54  
55  
56  
57  
58  
59  
60  
61  
62  
63  
64  
65



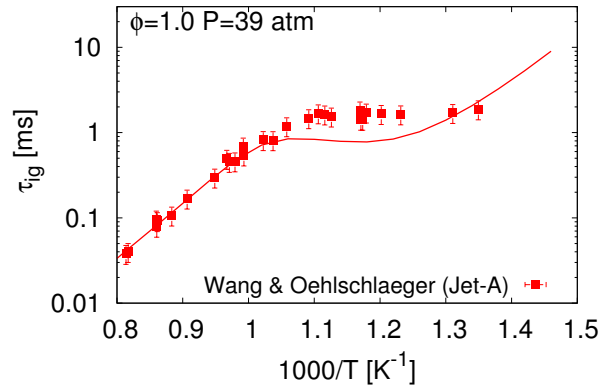
(a)  $\phi = 1$   $P = 20$  atm



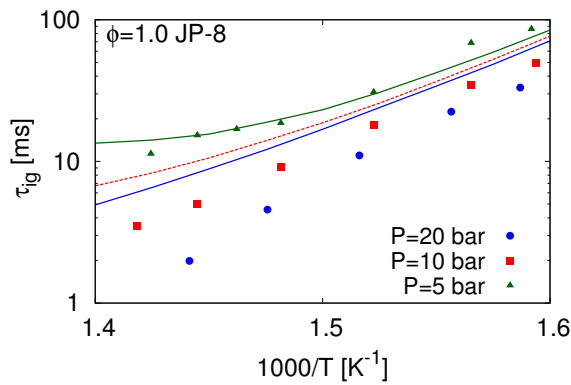
(b)  $\phi = 1$   $P = 20$  atm



(c)  $\phi = 1.0$   $P = 32\text{--}50$  atm



(d)  $\phi = 1.0$   $P = 39$  atm



(e) Pressure dependence at low temperatures

Figure 10: Ignition delay times of JP-8/Jet-A fuels at stoichiometric fuel/air equivalence ratios: Symbols - experimental data from Vasu *et al.* [41], Zhukov *et al.* [45], Wang and Oehlschlaeger [3], Valco *et al.* [46], and Dooley *et al.* [39]; lines - results from simulations.

1 At elevated pressures,  $P \sim 40$  atm, in Fig. 10(c), the  
2 computations show an excellent agreement with the ex-  
3 perimental data at high temperatures. However, at in-  
4 termediate temperatures,  $700 \text{ K} < T < 900 \text{ K}$ , in Fig. 10(d),  
5 the simulations predict shorter ignition delays, accompa-  
6 nied by an early transition into low temperature ignition  
7 regime (meaning a transition at higher temperatures) than  
8 that suggested by the experiments.

9 This is a manifestation of the simulations at inter-  
10 mediate temperatures showing similar dependence of igni-  
11 tion delays on pressure at all pressures, while the ex-  
12 periments suggest otherwise. At intermediate temper-  
13 atures, from their experiments, Wang and Oehlschlaeger  
14 noted a stronger dependence of ignition delays on pressures  
15 at lower pressures, and a weaker dependence at elevated  
16 pressures. To be specific, between pressures  $P \sim 11$  atm  
17 and  $P \sim 20$  atm, the measured ignition delays are 3 times  
18 longer at the lower pressure. In contrast, between pres-  
19 sures  $P \sim 20$  atm and  $P \sim 39$  atm, the measured ignition de-  
20 lays take similar values, within 10% difference between  
21 these two pressures.

22 It is not entirely unexpected that the computed igni-  
23 tion delays for  $\mathcal{S}_o$  show a similar pressure dependence at  
24 moderate and elevated pressures, since such a behavior was  
25 also observed at intermediate temperatures for the major  
26 components,  $n$ -dodecane (in Fig. S4(a)) and methylcyclo-  
27 hexane (in Fig. S5). Substantiating this trend, a sensitiv-  
28 ity analysis performed at  $P = 20$  and  $40$  atm for the fuel  
29 specific reactions (shown in Fig. S13 in the Supplementary  
30 materials) also reveals that the ignition delays are sensitive  
31 to nearly the same set of reactions, suggesting that similar  
32 kinetics are at play at those different pressures. In view  
33 of this discussion, it could be concluded that the weaker  
34 pressure dependence displayed by the experiments at ele-  
35 vated pressures for the jet fuel cannot be represented using  
36 the proposed surrogate mixture.

37 The ignition delays measured at different pressures in  
38 an RCM by Valco *et al.* [46] at low temperatures ( $T < 700 \text{ K}$ )  
39 are considered next (Fig. 10(e)). The computations agree  
40 with the measurements at the lowest pressure examined,  
41 while predicting longer ignition delays compared to the  
42 data at higher pressures. The predicted temperature de-  
43 pendence on ignition delays (*i.e.* the slope  $d\tau/dT$ ) fol-  
44 lows the experimental data at all pressures. However, the  
45 simulated ignition delays do not exhibit the strong de-  
46 pendence observed in the experimental data. Note that  
47 a similar weak dependence of the computed ignition de-  
48 lays on pressure was also observed for the major surrogate  
49 components,  $n$ -dodecane [56] (see Fig. S4(b)) and methyl-  
50 cyclohexane [57] (see Fig. S5) at low temperatures. The  
51 pressure dependence of the ignition delays of the jet fuel  
52 at low temperatures must be revisited when additional  
53 experimental data become available at those conditions,  
54 preferably from a different measurement facility, such as  
55 the shock tube.

#### 4.1.3. Fuel rich conditions

At richer conditions,  $\phi = 1.5$ , a comparison of the com-  
puted ignition delays against the experimental data from  
Wang and Oehlschlaeger [3] is shown in Fig. 11(a). A  
good agreement is seen at moderate to high temperatures,  
 $T > 760 \text{ K}$ . At lower temperatures, the simulations show  
longer ignition delays compared to the experiments, which  
could be explained by a similar trend shown by ignition  
delays of  $n$ -dodecane (see Fig. S11).

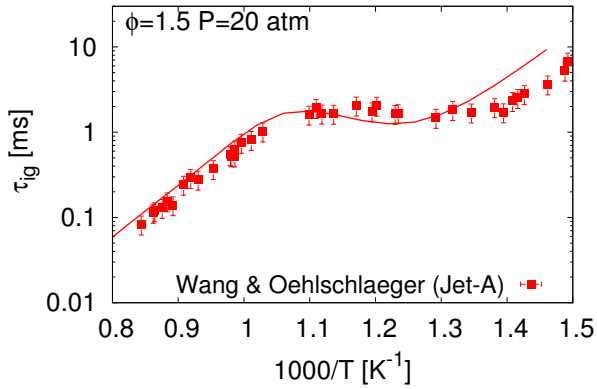
The simulations show an over-prediction compared to  
ignition delays at equivalence ratio of  $\phi = 2.0$  and high  
temperatures measured by Dean *et al.* [43] and Zhukov *et al.* [45] in Fig. 11(b). In the study of Dean *et al.* [43],  
the ignition delays were determined using chemilumines-  
cence from the shock tube side wall, and as pointed out by  
Horning *et al.* [106], measurements made at side wall loca-  
tions can result in artificially shortened observed ignition  
delay times for highly exothermic reactant mixtures. This  
could possibly explain the longer ignition delays predicted  
by the simulations in comparison to the experimental data  
of Dean *et al.* [43]. However, the recent measurements of  
Zhukov *et al.* [45] at  $P = 10$  atm show a modest agree-  
ment with the Dean *et al.* data, which makes the above  
explanation dubious.

Despite a very good agreement between the computed  
ignition delays and those measured at high temperatures  
by Wang and Oehlschlaeger at  $\phi = 1.5$  (see Fig. 11(a)),  
the results show an over-prediction compared to the data  
from Zhukov *et al.* at similar temperatures and pressures,  
but at  $\phi = 2.0$ . This suggests that the high temperature  
predictions of the reaction mechanism used are inadequate  
at very rich mixtures, such as  $\phi = 2.0$ , presumably due to  
the absence of an elaborate rich oxidation chemistry.

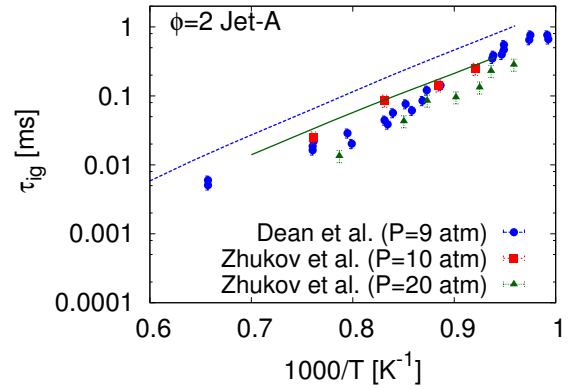
#### 4.1.4. Comparison with existing surrogate models

Ignition delays of jet fuels predicted using recent mod-  
els (2009–present) are shown in Fig. 12. Also shown in  
this figure are the ignition delays predicted using the ki-  
netic scheme used here with  $\mathcal{S}_o$  as the jet fuel surrogate.

While capturing high temperature ignition within the  
experimental uncertainties, the model proposed by Hon-  
net *et al.* [107] predicts ignition delays almost a factor  
of 3 shorter than the experiments at lower temperatures  
( $T < 900 \text{ K}$ ). The models by Dooley *et al.* [39] and Malewicky  
*et al.* [52] (UIC model) show longer ignition delays (factor  
of 2 and 1.5 respectively) compared to experiments at high  
temperatures. The predictions from Dooley *et al.* model  
agree with data from Vasu *et al.* [41] at moderate tempera-  
tures ( $750 \text{ K} < T < 900 \text{ K}$ ), while the Malewicky *et al.* model  
shows faster ignition delays (by almost a factor of 1.5) at  
those temperatures. The recent model by Kim *et al.* [35]  
(UMI model) shows good agreement with the data from  
Vasu *et al.* [41] at high and moderate temperatures, while  
predicts longer ignition delay by almost a factor of 2 at  
 $900 < T < 1100 \text{ K}$ . It can be seen that among all these mod-  
els, the predictions obtained using the present model show



(a)  $\phi = 1.5$   $P = 20$  atm



(b)  $\phi = 2$   $P = 10, 20$  atm

Figure 11: Ignition delay times of JP-8/Jet-A fuels at rich fuel/air equivalence ratios: Symbols - experimental data from Wang and Oehlschlaeger *et al.* [3]; lines - results from simulations.

the best agreement with the available experimental data at this condition.

In summary, the simulations show a good agreement with experimental ignition delay data at high temperatures, at different equivalence ratios, and atmospheric to elevated pressures, excepting at very rich conditions where the results predict longer ignition times than the experiments. The predictions at low and moderate temperatures are satisfactory for all available experimental data sets, and show a better agreement with the experiments at stoichiometric conditions (at  $P = 20$  atm) than the existing surrogate models (see Fig. 12). The simulations underpredict ignition delays at high pressures ( $P \sim 40$  atm) and moderate temperatures, which could be attributed to the pressure dependence of the ignition delays of the components themselves.

#### 4.2. Shock tube oxidation

Mole fractions of the stable species produced during the oxidation of Jet-A fuel (POSF 4658) were measured by Malewicki *et al.* [52] and Dooley *et al.* [40] in a heated high pressure single pulse shock tube, at fixed reaction times, as a function of reactor temperature. Their experimental data was obtained for Jet-A/ $O_2$ /argon mixtures at moderate to high temperatures,  $T = 890$ – $1680$  K, varied pressures,  $P = 16$ – $26$  atm, and equivalence ratios,  $\phi = 0.46, 1.01, 1.85$ . The reaction time at which the mole fractions were reported is defined as the time duration between the initial pressure rise due to the incident shock reflection and the time to reach 80% of the maximum pressure rise, and varied between 1.34–3.25 ms at different temperatures.

For temperatures  $T < 1350$  K, the uncertainty in measured temperatures is estimated at  $< 1\%$  and for  $T > 1350$  K, this value is  $< 2\%$ . The uncertainty for species measurements is estimated to be  $\pm 10\%$ . The experimental set

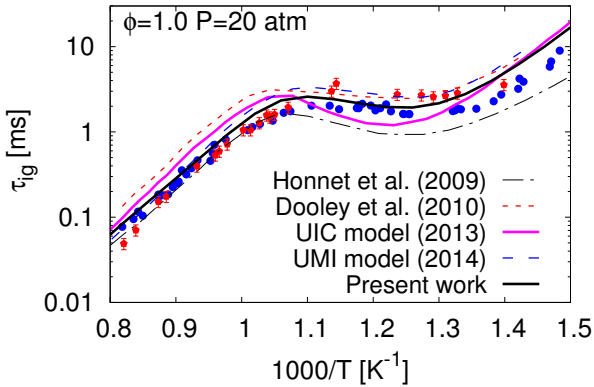


Figure 12: Ignition delay times of JP-8/Jet-A fuels: Symbols - experimental data from Vasu *et al.* [41] (pink diamonds) and Wang and Oehlschlaeger [3] (blue circles); lines - predictions using existing surrogate models: Honnet *et al.* [107], Dooley *et al.* [39], UIC model [52], UMI model [35]; *Present work*—predictions using the present reaction scheme (section 3.4) with  $\mathcal{S}_o$  (Table 3) as fuel.

up is modeled here using constant volume simulations at the exact pressures, temperatures, and reaction times, reported in the data sets. The real jet fuel is modeled using  $\mathcal{S}_o$  (Table 3), using the experimental equivalence ratios.

#### 4.2.1. Lean oxidation

The results of the computations are shown in Fig. 13 for the lean oxidation case along with the experimental data. The simulations and the experiments show a modest agreement for the oxidizer, carbon oxides, small alkanes, alkenes, allene, and propyne in Figs. 13(a)–13(f). There is little reactivity at  $T < 1000$  K ( $< 5\%$  fuel is consumed) while CO and CO<sub>2</sub> builds up at higher temperatures. A reaction flux analysis that describes the fuel decay pathways at high temperatures is presented in section S3.1.1. This analysis further reveals that, while the reactivity of *n*-dodecane is similar in the neat fuel and the surrogate mixture, both methylcyclohexane and *m*-xylene in the surrogate fuel show an enhanced reactivity compared to neat fuel oxidation (see Fig. S6).

**Higher hydrocarbons.** In Fig. 13(g), the computations show a satisfactory agreement with the experiments for 1,3-butadiene and but-1-en-3-yne, as well as a good agreement for benzene in Fig. 13(j), however this deteriorates for larger alkenes and toluene in Figs. 13(h)–13(j). The kinetic model cannot be expected to predict these species in good detail, since these products depend on the chosen components for the surrogate fuel. For instance, isoprene and 1,3-pentadiene are produced from the branched heptenyl radicals which are intermediates of methylcyclohexane oxidation, and hence produced in large amounts from the proposed surrogate mixture, which contains 48.5% (by mole) of methylcyclohexane. Following a similar argument, 1-pentene is produced in large amounts compared to the experiments, since this is a primary product of *n*-dodecane oxidation, which is present in significant amounts in the surrogate fuel. In view of this, the amounts of 1-hexene and heptene predicted by the simulations showing a modest agreement with the experiments should also be considered with caution.

Due to the presence of a wide range of hydrocarbons in the real fuel, specific large hydrocarbons intermediates are not formed in significant amounts during the oxidation of the fuel. Differences in amounts of higher carbon intermediates were also noted by Dooley *et al.* [40] when comparing their surrogate with the real fuel oxidation intermediates in the same shock-tube experiment. These differences could therefore be attributed more to the simple surrogate representation employed here than to the inaccuracy of the proposed kinetic scheme for the surrogate.

#### 4.2.2. Stoichiometric and rich oxidation

For the case of stoichiometric and rich oxidation, the oxidizer profiles measured in the experiments and the simulations in Fig. 14 show a good agreement, except for slower oxidizer consumption compared to the experiments

at  $T = 1300$ – $1500$  K and  $T > 1300$  K, respectively. At those temperatures, the computed results for small carbon ( $< C_4$ ) intermediates also show a shifted profile compared to the experiments, nonetheless, showing overall good agreement at other temperatures in Figs. 15, S7, and S8. A similar shift was also observed when comparing profiles of neat *n*-dodecane oxidation with shock tube data at stoichiometric and rich conditions at these temperatures (see Fig. S9) and at rich conditions during *m*-xylene oxidation (see Fig. S10).

Malewicki *et al.* [108, 109] note that revisions to C<sub>1</sub>–C<sub>2</sub> chemistry from Gudiyaella *et al.* [110] result in better O<sub>2</sub> decay profiles in their simulations of iso-octane and *n*-dodecane oxidation when comparing to shock tube data. However, these revisions provided in Table S5 of Malewicki and Brezinsky [109], when incorporated in the proposed scheme, result in little differences to the simulated oxidizer profiles shown in Fig. 14. The predictions for species concentration profiles in *n*-dodecane and *m*-xylene oxidation at these conditions must be improved in order to achieve better agreement for the surrogate.

For the larger carbon ( $> C_4$ ) intermediates, the significant differences observed between the experiments and the simulations (see Figs. S7 and 15(e)) could be explained following the argument presented in the previous sub-section. In summary, the simulations demonstrate the ability to predict the amounts of smaller hydrocarbons satisfactorily in comparison to the experimental data. A reaction flux analysis to identify pathways responsible for the production of different intermediate hydrocarbon intermediates is presented in the Supplementary materials, section S3.1.2.

#### 4.3. Variable Pressure Flow Reactor

Dooley *et al.* [39] considered the oxidation of a specific Jet-A fuel (POSF 4658) in a variable pressure flow reactor with initial 0.3 mol% Carbon at  $\phi = 1.0$  in a mixture of fuel/O<sub>2</sub>/N<sub>2</sub>, pressure  $P = 12.5$  atm, at low to moderate temperatures, 550–1050 K, and a fixed residence time,  $\tau = 1.8$  s. The use of dilute conditions ensure that the local and total heat release depart from the reactor temperature by less than 50 K, and therefore an adiabatic flow reactor model is valid [40]. A comparison between the simulated species concentrations (at time  $\tau = 1.8$  s) and the experimental data from Dooley *et al.* is shown in Fig. 16.

The reactivities of the surrogate fuel and the real jet fuel start at  $T \sim 560$  K. At these low temperatures, the simulations show an increased reactivity compared to the real fuel, indicated by a larger depletion of oxidizer in Fig. 16(a) and higher concentrations of CO in Fig. 16(b). The increased reactivity trend exhibited by the simulations continue into the NTC regime of oxidation for temperatures 625–700 K. The over-prediction of CO is also observed when comparing against experimental data from Natelson *et al.* [47] at a lean equivalence ratio ( $P = 8$  bar, residence time = 0.120 ms, 80% N<sub>2</sub> dilution) and low temperatures (see Fig. 17).

Differences in amounts of CO were also observed in comparison to experiments for neat *n*-dodecane oxidation

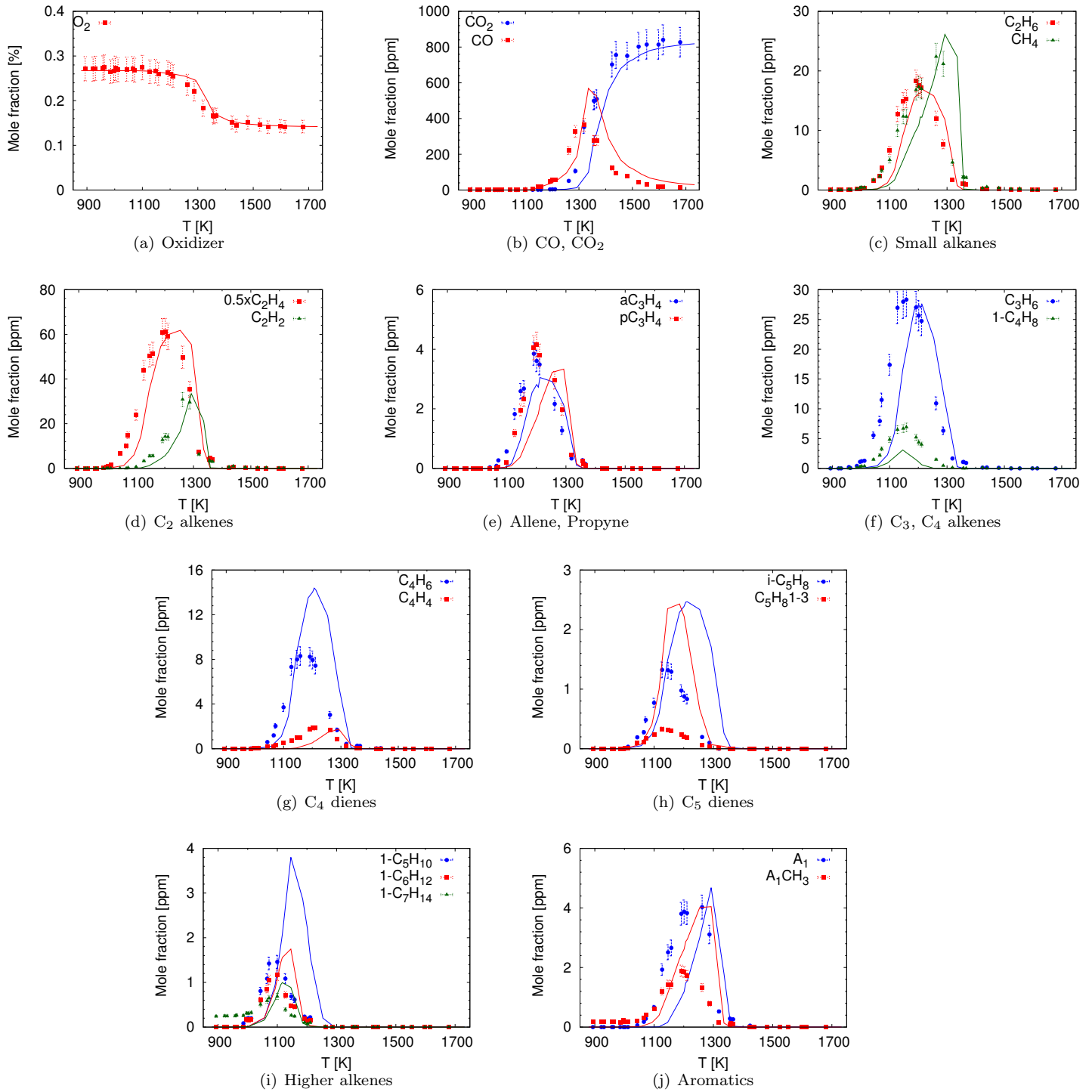


Figure 13: Shock tube oxidation of Jet-A (POSF 4658): Symbols - experimental data from Malewicki *et al.* [52] at  $\phi = 0.46$ ,  $P = 16\text{--}27$  atm, reaction times = 1.34–3.36 ms; lines - results from simulations.

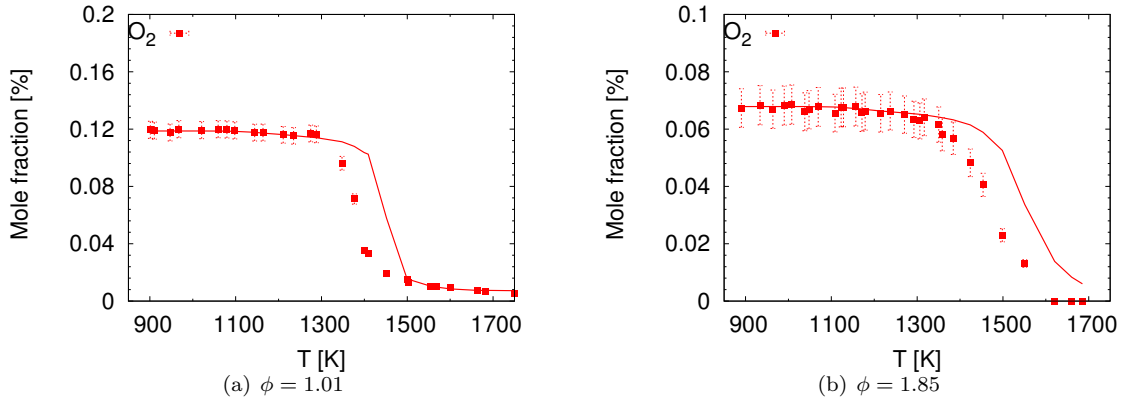


Figure 14: Shock tube oxidation of Jet-A (POSF 4658): Symbols - experimental data from Malewicki *et al.* [52] at  $\phi = 1.01$  and 1.85,  $P = 16\text{--}27$  atm, reaction times = 1.34–3.36 ms; lines - results from simulations.

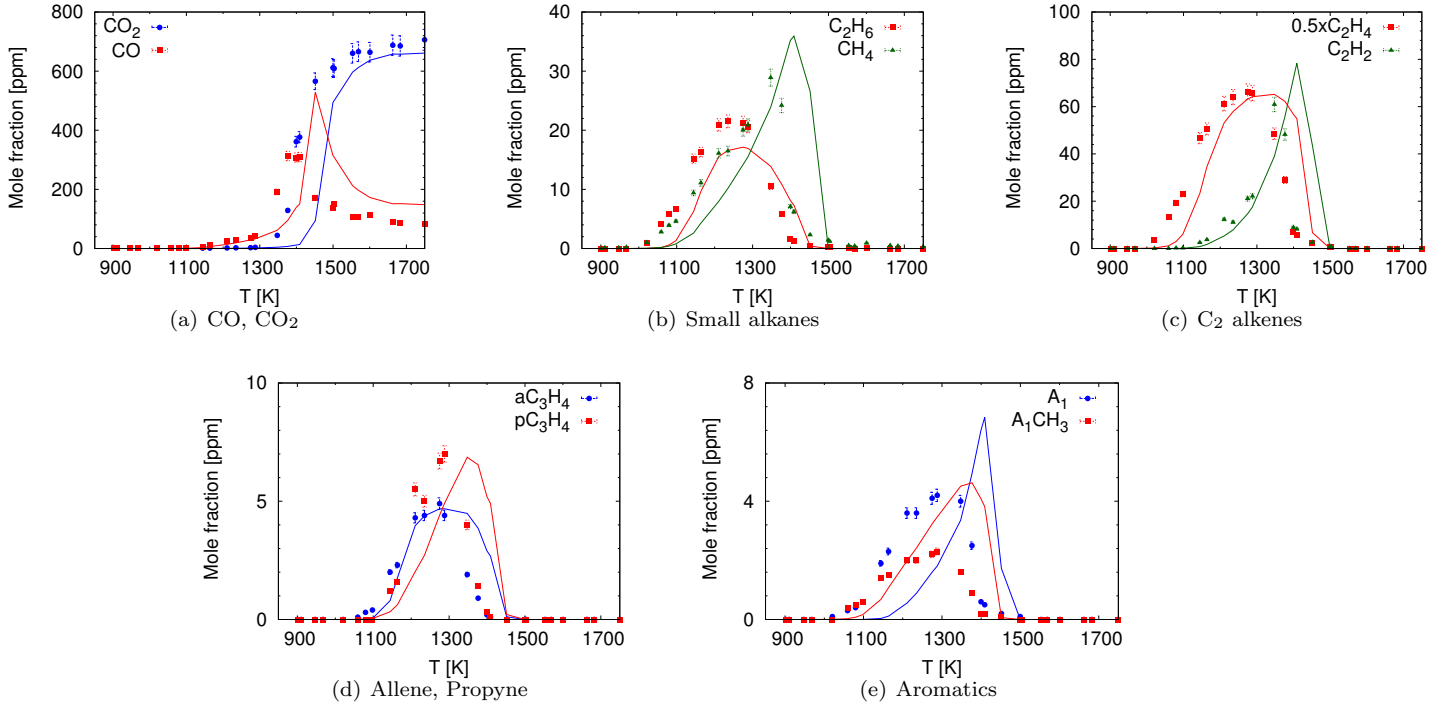


Figure 15: Shock tube oxidation of Jet-A (POSF 4658): Symbols - experimental data from Malewicki *et al.* [52] at  $\phi = 1.01$ ,  $P = 16\text{--}27$  atm, reaction times = 1.34–3.36 ms; lines - results from simulations.

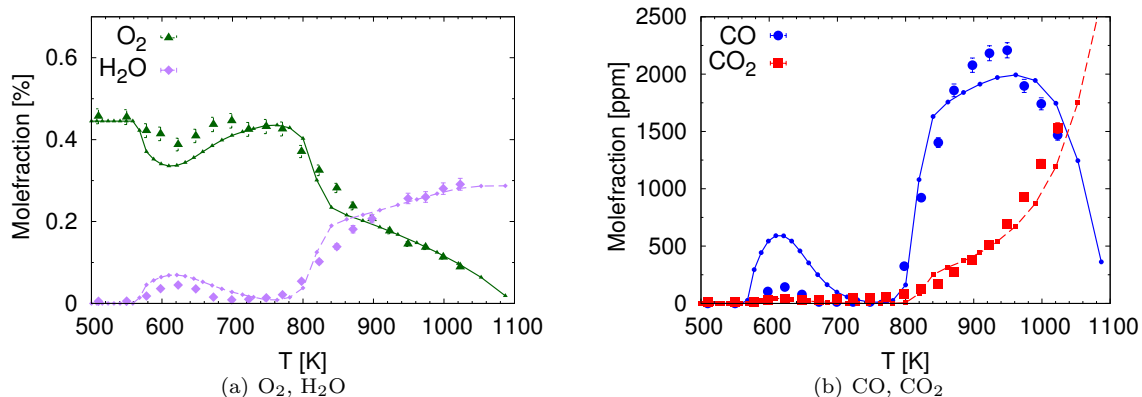


Figure 16: Concentration profiles of major species during the oxidation of a specific Jet-A fuel (POSF 4658) in a variable pressure flow reactor with initial 0.3 mol% Carbon at  $\phi = 1.0$  in a mixture of fuel/ $O_2/N_2$ , pressure  $P = 12.5$  atm, at low to moderate temperatures,  $550\text{ K} < T < 1050\text{ K}$ , and a fixed residence time,  $\tau = 1.8\text{ s}$ : Symbols - (a,b) experimental data from Dooley *et al.* [39]; Uncertainties in the measurements are:  $O_2 < 4\%$ ,  $H_2O < 5\%$ ,  $CO < 3\%$ ,  $CO_2 < 3\%$ , Solid lines - results from simulations.

at low temperatures (see Fig. S12). Therefore, it appears that improvements to *n*-dodecane kinetics for these conditions could lead to better agreement for the surrogate as well. This potentially involves changes to both thermodynamic properties of species participating in low temperature chemistry and rate rules employed for reaction classes important at low temperatures, as suggested by Bugler *et al.* [111] and Cai *et al.* [112].

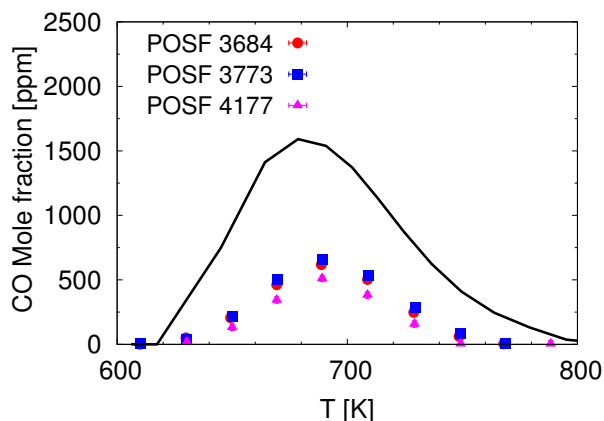


Figure 17: Reactivity map of different jet fuels at low temperature signified by CO mole fraction at low temperatures: Symbols - experiments from Natelson *et al.* [47], lines - results from simulations.

Between 700–760 K, there is reduced reactivity compared to lower and higher temperatures with little oxidizer consumption and product formation in Figs. 16(a) and 16(b). As temperature is increased above 780 K, the oxidation behavior transitions to high temperature ignition regime, with increasing reactivity as at higher temperatures. The simulated profiles predict the transition into high temperature ignition regime accurately, following the experiments. The concentrations of  $CO_2$  and  $H_2O$  show a good agreement with the experiments at  $T > 750\text{ K}$ ,

and the CO concentrations show deviations up to 10%.

*Reactivity of surrogate fuel components.* The reactivity chart of the different fuels in the surrogate mixture shown in Fig. 18(a) clearly display regions of low, moderate, and high temperature reactivity for the different fuel components, although to different extents. At low temperatures 560–625 K, *n*-dodecane and methylcyclohexane are consumed entirely, while almost 60% of *m*-xylene is left unreacted. In the NTC ignition regime 625–760 K, the fuels are consumed to a lesser extent due to decreased reactivity and thereafter entirely consumed in the high temperature ignition regime ( $T > 780\text{ K}$ ).

Comparing the reactivity chart of the individual neat fuels (shown in Fig. 18(b)) with that of the fuels in the surrogate mixture (Fig. 18(a)), some observations can be made. Neat *n*-dodecane shows an early reactivity at low temperatures (by about 20 K) compared to that in the mixture, and a higher reactivity at moderate temperatures (650–800 K), while the high temperature reactivity is similar for the pure fuel as well as the mixture, with *n*-dodecane entirely consumed. This suggests that the low and intermediate temperature reactivity of the *n*-dodecane fuel component is reduced in the surrogate mixture due to the presence of methylcyclohexane and *m*-xylene, while the high temperature reactivity is largely unaffected. This is also confirmed by the reactivity of methylcyclohexane at low and moderate temperatures. Pure methylcyclohexane shows delayed reactivity at low temperatures (by about 50 K) and a slower reactivity at moderate temperatures compared to that in the mixture, while its reactivity as a pure fuel as well as in the mixture are similar at high temperatures.

The differences in reactivity are marked between the oxidation of pure *m*-xylene and that of *m*-xylene in the surrogate mixture. For pure *m*-xylene, no reactivity is observed at  $T < 1000\text{ K}$ , whereas reactivity at low and moderate temperatures is clearly displayed for *m*-xylene oxi-

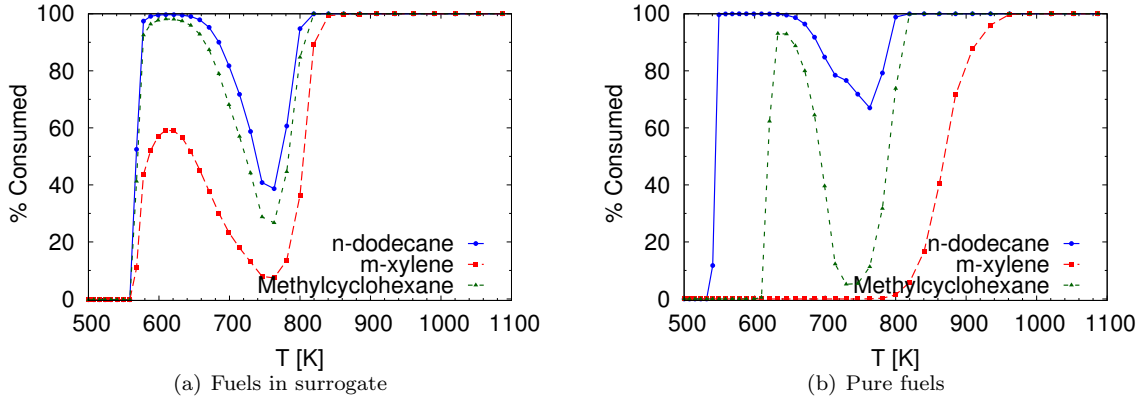


Figure 18: Normalized fuel consumption for (a) components in surrogate mixture and (b) neat (or pure) fuel oxidation. Lines with points are results from simulations performed at the experimental conditions of Fig. 16.

dation in the surrogate mixture in Fig. 18(a). This suggests that the radicals produced from the oxidation of *n*-dodecane and methylcyclohexane lead to an increased reactivity of *m*-xylene at these moderate and low temperatures.

#### 4.4. Laminar flame speeds

##### 4.4.1. Comparison with experimental data

Ji *et al.* [48] measured laminar flame speeds of JP-8 fuel at atmospheric pressure and at an unburnt temperature of  $T_u = 403$  K. At similar conditions as well at higher pressures and higher unburnt temperatures, Hui *et al.* [49], Singh *et al.* [50], Kumar *et al.* [51], and Dooley *et al.* [40] have also measured laminar flame speeds for Jet-A fuels. The simulated flame speeds are compared with these experimental data in Fig. 19.

In Fig. 19(a), the flame speed predictions at atmospheric pressure and a preheat temperature of  $T_u = 403$  K closely follow those reported by Hui *et al.* [49] at most of the equivalence ratios and lie within the variability of the rest of the experimental data. The simulations agree with the Ji *et al.* data at rich equivalence ratios, but show differences compared to the data reported by Dooley *et al.* [40] and Kumar *et al.* [51] at both unburnt temperatures,  $T_u = 403, 470$  K.

Note that the unstretched laminar flame speeds reported by Hui *et al.* and Ji *et al.* were obtained by a non-linear extrapolation of the flame speed versus strain rate curve to zero-stretch rate, whereas Kumar and Sung and Dooley *et al.* used a linear extrapolation. This could explain the differences between the experimental data sets for rich fuel/air mixtures at  $T_u = 403$  K. Since the simulations agree with the more accurate non-linearly extrapolated laminar flame speed data at  $T_u = 403$  K, this lends credibility to the computed results. It could be surmised that the simulations would agree with non-linearly extrapolated laminar flame speeds at the higher unburnt temperature ( $T_u = 470$  K) as well. At higher pressures, the simulations reproduce the flame speed measurements of

Hui *et al.* within their reported uncertainties, as shown in Fig. 19(b).

##### 4.4.2. Adiabatic temperature and flame speed correlations

Ji *et al.* [113] showed that accurate estimates for the adiabatic flame temperatures and flame speeds of mixtures of *n*-dodecane/methylcyclohexane and *n*-dodecane/toluene can be obtained from the corresponding values of the individual fuel components, based on the analysis proposed by Hirasawa *et al.* [114] for *n*-butane/toluene mixtures.

From the analysis presented by Ji *et al.* [113] and Hirasawa *et al.* [114],

$$T_{ad}^{mix} = \frac{\sum_{i=1}^{n_{fuels}} X_i N_i T_{ad}^i}{\sum_{i=1}^{n_{fuels}} X_i N_i} \quad \text{and} \quad (3)$$

$$\log S_L^{mix} = \sum_{i=1}^{n_{fuels}} \left\{ X_i N_i \frac{T_{ad}^i}{T_{ad}^{mix}} \log S_L^i \right\}, \quad (4)$$

where  $X_i$  is the mole fraction of the  $i^{th}$  component in the fuel mixture,  $N_i$  the total number of moles of products (obtained from the equilibrium composition),  $T_{ad}^i$  is the adiabatic flame temperature, and  $S_L^i$  is the laminar flame speed of the neat fuel  $i$  (as a function of  $\phi$ ).

These relations are now used for the ternary mixture of *n*-dodecane/*m*-xylene/methylcyclohexane proposed as the jet fuel surrogate in this work (given in Table 3). The estimated adiabatic flame temperatures show an excellent agreement with the computed values to within  $<0.1\%$  at all equivalence ratios in Fig. 20(a). The estimated and computed flame speeds show a good agreement, with the maximum difference being 8% for the rich equivalence ratios, suggesting that kinetic coupling among fuels have little effect on flame speeds, as noted by Ji *et al.* [113].

1  
2  
3  
4  
5  
6  
7  
8  
9  
10  
11  
12  
13  
14  
15  
16  
17  
18  
19  
20  
21  
22  
23  
24  
25  
26  
27  
28  
29  
30  
31  
32  
33  
34  
35  
36  
37  
38  
39  
40  
41  
42  
43  
44  
45  
46  
47  
48  
49  
50  
51  
52  
53  
54  
55  
56  
57  
58  
59  
60  
61  
62  
63  
64  
65

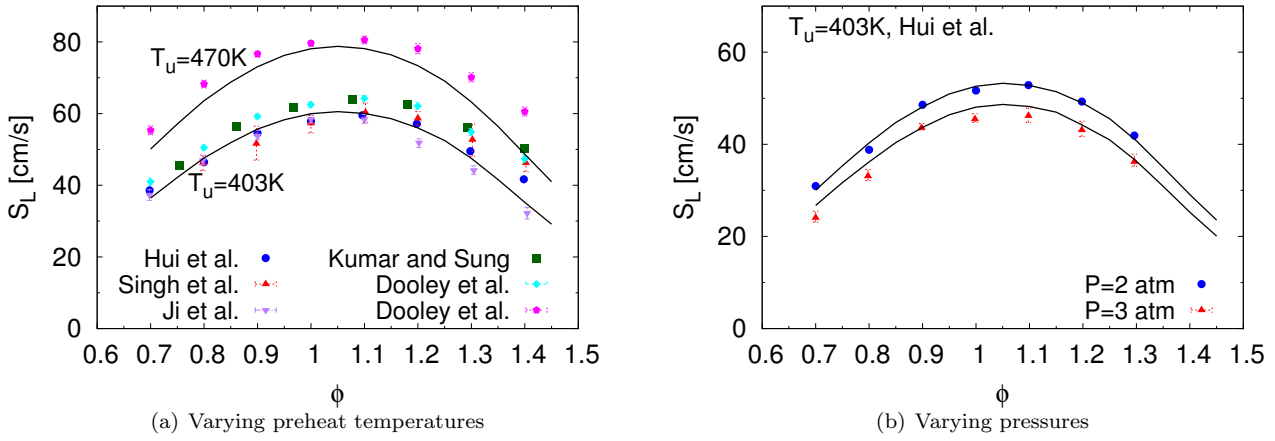


Figure 19: Laminar flame speeds of jet fuels: Symbols - experimental data for jet fuels from Ji *et al.* [48], Kumar *et al.* [51], Hui *et al.* [49], Singh *et al.* [50]; lines - results from simulations.

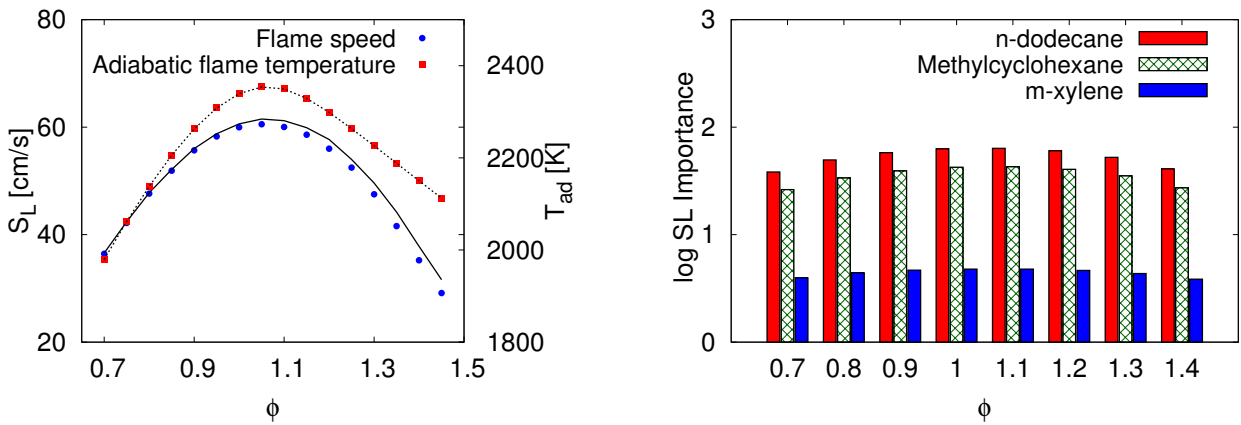


Figure 20: (a) Laminar flame speeds and adiabatic flame temperatures for the proposed jet fuel surrogate estimated using correlations (3), (4) based on individual components, and (b) importance of different fuel components towards the flame speeds of the surrogate mixture in log scale, as a function of equivalence ratio.

The quantities within curly parentheses in equation (4) are indicative of the importance of the different fuels towards the (logarithm of) flame speed of the mixture, and these are plotted in Fig. 20(b). This bar chart shows that the importance values of *n*-dodecane and methylcyclohexane are similar at all equivalence ratios, while that of *m*-xylene is less than half of the other two fuels. This suggests that it is important to accurately predict the flame speeds of *n*-dodecane and methylcyclohexane in order to predict that of the mixture reliably. Similar conclusions are obtained when considering the importance of different fuel components towards the maximum concentrations of H, O, and OH radicals produced in premixed flames at different equivalence ratios (see section S6 in Supplementary materials).

#### 4.5. Species profiles in flames

The chemical structure of an atmospheric burner stabilized rich ( $\phi = 1.7$ ) premixed kerosene flame was investigated by Douté *et al.* [23]. The mole fraction profiles of major species and products were measured using gas chromatography. The simulations are compared to their experimental data in Fig. 21.

The temperature profile is prescribed from the experiments in the present simulation. The initial conditions in terms of species mole fractions and injection velocity for the premixed kerosene flame need to be adjusted from the experimental data, as the surrogate differs from the average formula used by Douté *et al.* [23] (assumed to be  $C_{11}H_{22}$ ). Conserving the element mass flux between the simulations and experiments results in the following constraints on the mass fractions of the reactants and the injection velocity used in the simulations (denoted by primed quantities) [38]:

$$v' = v \left( \frac{n_C}{n_C'} X_F + X_{O_2} + X_{N_2} \right) \quad (5)$$

$$X_F' = \frac{n_C}{n_C'} \frac{v}{v'} X_F \quad (6)$$

$$= \frac{n_H}{n_H'} \frac{v}{v'} X_F \quad (7)$$

$$X_{O_2}' = \frac{v}{v'} X_{O_2} \quad (8)$$

$$X_{N_2}' = \frac{v}{v'} X_{N_2} \quad (9)$$

where  $X_F$ ,  $X_{O_2}$ , and  $X_{N_2}$  are the mole fractions of kerosene, oxygen, and nitrogen, respectively, and  $v$  is the injection velocity used in the experiment,  $n_C$  and  $n_H$  are the number of carbon and hydrogen atoms in the assumed molecular formula of the kerosene fuel. It is not possible to satisfy eq. (7) here, since the H/C ratio for the present surrogate is different from that of the fuel studied experimentally. Therefore, the initial conditions are obtained by conserving the mass flux of carbon (eq. (6)) between the experiments and the simulations.

The major products CO, CO<sub>2</sub>, and H<sub>2</sub> (in Fig. 21(a)) are well predicted by the simulations. In Fig. 21(b), the

oxidizer is consumed faster than the experiments starting 4 mm from the burner, and correspondingly, the amount of H<sub>2</sub>O is over-predicted compared to the experiments. The faster consumption of O<sub>2</sub> also correlates with the early decay of small hydrocarbon intermediates ( $\leq C_3$ ) in Figs. 21(c)–21(e). While the amounts of allene and propyne are under-predicted by the simulations, the concentration of benzene (C<sub>6</sub>H<sub>6</sub>) is captured well.

The agreement between the experiments and simulations remains satisfactory in view of the significant uncertainty in the temperature profile measured in the experiments (about  $\pm 100$  K). Further, the H/C ratio of the fuel used in the experiment and the present surrogate is different, which could also be important to explain the differences observed in Fig. 21.

In summary, in this section, the proposed jet fuel surrogate ( $\mathcal{S}_o$ ) and the kinetic mechanism to describe its oxidation have been evaluated comprehensively by comparing against available experimental data. Thus, the ability of the surrogate to predict the real fuel combustion characteristics has been characterized in detail. Further, the importance of the different surrogate fuel components towards predicting global combustion characteristics have also been discussed. The validation tests conducted in this study show that the surrogate  $\mathcal{S}_o$ , which is representative of the average jet fuel, and its kinetic mechanism is able to capture combustion characteristics in several cases satisfactorily.

## 5. Conclusions

A flexible and evolutive component library framework has been proposed to derive short chemical mechanisms with only the necessary kinetics for the desired surrogate mixture. Using these accurate and compact kinetic models, an extensive evaluation of several surrogate mixtures in emulating the combustion kinetic behavior of the real fuel can be conducted. Thereby, the best choice of surrogate components among the several mixtures typically considered as surrogates for real fuels could be identified.

The concept has been demonstrated using a multi-component reaction scheme developed from our previous kinetic modeling efforts [54–57], by reorganizing it in the form of a parent mechanism containing sub-mechanisms of several component fuels, thanks to its compact size and modular mechanism assembly. A script to extract a chemical mechanism for a surrogate mixture, the kinetics of whose individual components are described in this parent chemical mechanism, is available online [69] as well as in the Supplementary materials.

Note that the component library approach described in this article can be applied, in principle, to any reaction mechanism. Nevertheless, the process of reorganizing the multi-component reaction scheme into a library of component sub-mechanisms will be readily feasible for a compact mechanism assembled in a modular fashion with no direct

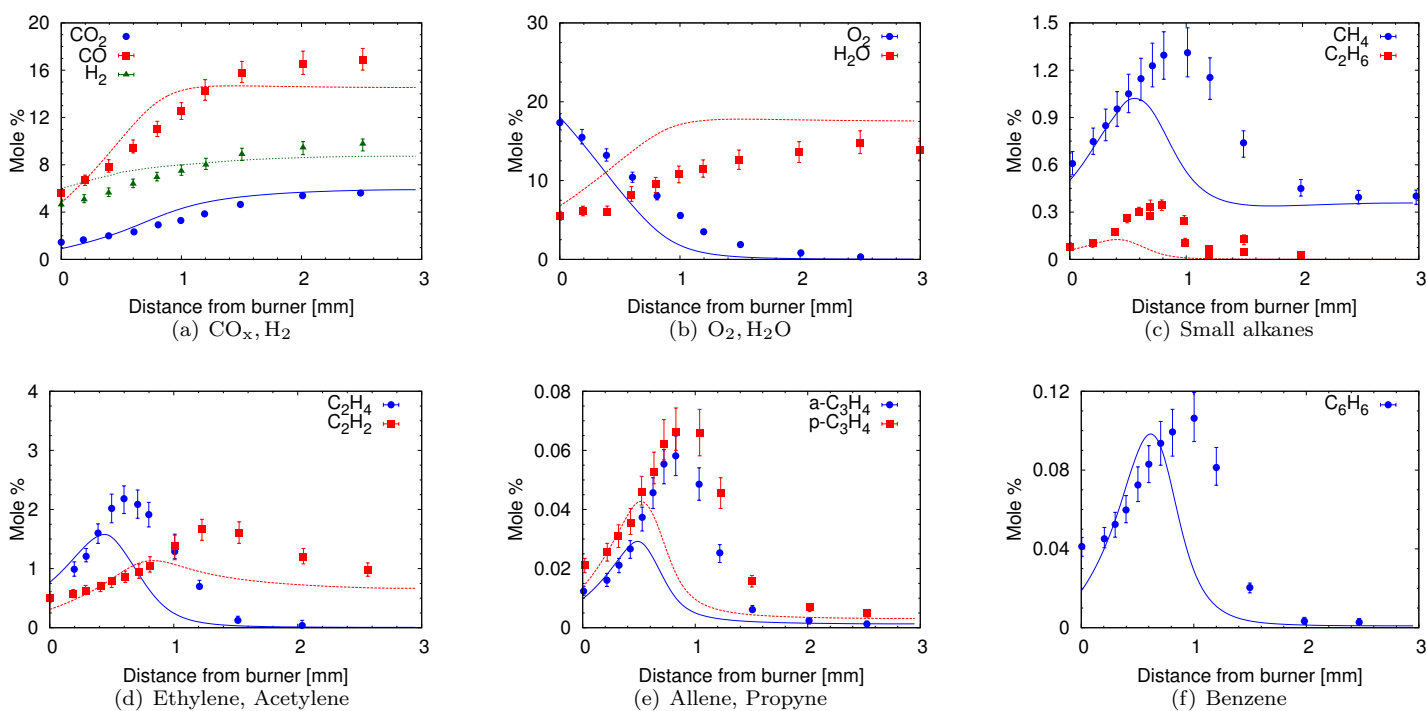


Figure 21: Species profiles in a burner stabilized flame; Symbols - experiments from Doute *et al.* [23]; lines - results from simulations. The temperature profile is prescribed from the experiment in the computations.

cross-reactions between heavy molecules. These criteria are met by the multi-component kinetic scheme [57] that was used to demonstrate the component library framework.

This parent multi-component reaction mechanism has been characterized extensively for the component kinetic description and also possesses a compact size (369 species and 2691 reactions, counting forward and reverse reactions separately). Hence, this kinetic scheme is accurate and reliable as well as amenable to chemical kinetic analysis. This reaction mechanism describes the kinetics of several substituted aromatics [55], *n*-dodecane [56], and methylcyclohexane [57], and has the capability to describe the oxidation of *n*-heptane and iso-octane, which are all important as components of transportation fuel surrogates. The ability to predict oxidation at low through high temperatures for a number of molecular species is another highlight of this kinetic model, which is important for controlling combustion in the context of using jet fuels in diesel and HCCI type engines. Furthermore, the well-validated aromatic chemistry makes this reaction mechanism appropriate for assessing the formation of pollutants.

This component library based re-arrangement of the multi-component reaction mechanism [57] makes it possible to extract reaction schemes for many hydrocarbon combinations. These kinetic mechanisms can then be used to assess potential surrogates for real fuels, such as Fischer-Tropsch, diesel, and gasoline fuels extensively. To give an example, the applicability of the component library frame-

work has been displayed for jet fuel surrogates in this work. A jet fuel surrogate is defined using a constrained optimization approach to contain 30.3% *n*-dodecane, 21.2% *m*-xylene, and 48.5% methylcyclohexane (mole %). The kinetics of this surrogate mixture are then extracted from the multi-component reaction mechanism described above using the component library approach. Thereafter, the predictive capabilities of the surrogate and the kinetic model are assessed extensively at low to high temperatures in well studied experimental configurations, such as shock tubes, rapid compression machines, premixed flames, and flow reactors.

Detailed validation has been conducted on a variety of data sets, showing good agreement in most cases. In fact, the ignition delays predictions compared to experiment data from low to high temperatures at stoichiometric conditions (at  $P = 20$  atm) show the best agreement among existing surrogate models. In a few cases, the simulations showed significant differences compared to experiments, and the discrepancies have been traced to either the inadequacy of the chosen components in the surrogate mixture or deficiencies in the predictions from component kinetics. The simulations also predict the experimental measurements of species profiles in flow reactors at high temperatures as well as laminar flame speeds accurately.

The reaction mechanism valid from low to high temperatures, which has been used to obtain the results shown in this work, as well as the mechanism applicable at high temperatures only, along with the thermodynamic and trans-

port properties are available as a part of the Supplementary materials.

## Acknowledgements

The first author gratefully acknowledges support from the New Faculty Initiation Grant, Project no. MEE/15-16/845/NFIG offered by Indian Institute of Technology Madras. The first and the second author acknowledge funding by AFOSR and NASA, in addition to support by SERDP under Grant WP-2151 with Dr. Robin Nissan as the program manager. The second author also acknowledges support by the European Union as part of the project "DREAMCODE" (Grant no. 620143) within the Clean Sky Joint Undertaking. This material is also based upon work supported by the National Science Foundation Grant #BRIGE - 1342362.

## References

- [1] J. C. Guibet, E. Faure-Birchem, Fuels and engines, Editions Technip Paris (1999) vol. 1.
- [2] M. Colket, T. Edwards, S. Williams, N. P. Cernansky, D. L. Miller, F. Egolfopoulos, P. Lindstedt, K. Seshadri, F. L. Dryer, C. K. Law, D. Friend, D. B. Lenhart, H. Pitsch, A. Sarofim, M. Smooke, W. Tsang, Development of an experimental database and kinetic models for surrogate jet fuels, in: 45<sup>th</sup> AIAA Aerospace Sciences Meeting and Exhibit, 2007, pp. 2007-770.
- [3] H. Wang, M. A. Oehlschlaeger, Autoignition studies of conventional and fischer-tropsch jet fuels, Fuel 98 (2012) 249-258.
- [4] K. Henz, Survey of jet fuels procured by the defense energy support center 1990-1996, Tech. rep., Defense Logistics Agency, Ft Belvoir, VA (1998).
- [5] T. Edwards, Kerosene fuels for aerospace propulsion-composition and properties, 38<sup>th</sup> AIAA/ASME/SAE/ASEE Joint Propulsion Conference & Exhibit AIAA 2002-3874.
- [6] T. Edwards, L. Q. Maurice, Surrogate mixtures to represent complex aviation and rocket fuels, J. Prop. Power 17 (2000) 461-466.
- [7] O. J. Hadaller, J. M. Johnson, World fuel sampling program, Report no. 647, Coordinating Research Council (2006).
- [8] L. M. Shafer, R. C. Striebich, J. Gomach, T. Edwards, Chemical class composition of commercial jet fuels and other specialty kerosene fuels, AIAA (2006) 2006-7972.
- [9] T. Edwards, C. Moses, F. Dryer, Evaluation of combustion performance of alternative aviation fuels, 46<sup>th</sup> AIAA/ASME/SAE/ASEE Joint Propulsion Conference & Exhibit 2010-7155.
- [10] Defense Energy Support Centre, Petroleum Quality Information systems, Annual Report, <http://www.desc.dla.mil/DCM/Files/2004PQISreportsmall.pdf> (2008).
- [11] T. Edwards, Jet fuel composition, Jet Fuel Toxicology.
- [12] P. Dagaut, M. Cathonnet, The ignition, oxidation, and combustion of kerosene: A review of experimental and kinetic modeling, Prog. Energy. Combust. Sci. 32 (1) (2006) 48-92.
- [13] C. Guéret, M. Cathonnet, J.-C. Boettner, F. Gaillard, Experimental study and modeling of kerosene oxidation in a jet-stirred flow reactor, Symposium (International) on Combustion 23 (1) (1991) 211-216.
- [14] S. Zabarnick, Chemical kinetic modeling of jet fuel autoxidation and antioxidant chemistry, Ind. Eng. Chem. Res. 32 (6) (1993) 1012-1017.
- [15] P. Dagaut, M. Reuillon, J.-C. Boettner, M. Cathonnet, Kerosene combustion at pressures up to 40 atm: experimental study and detailed chemical kinetic modeling, Symp. (Int.) on Combustion 25 (1) (1994) 919-926.
- [16] R. P. Lindstedt, L. Q. Maurice, Detailed chemical-kinetic model for aviation fuels, J. Prop. Power 16 (2) (2000) 187-195.
- [17] P. Dagaut, On the kinetics of hydrocarbons oxidation from natural gas to kerosene and diesel fuel, Phys. Chem. Chem. Phys. 4 (11) (2002) 2079-2094.
- [18] A. Violi, S. Yan, E. G. Eddings, A. F. Sarofim, S. Granata, T. Faravelli, E. Ranzi, Experimental formulation and kinetic model for JP-8 surrogate mixtures, Combustion Science and Technology 174 (11-12) (2002) 399-417.
- [19] C. J. Montgomery, S. Cannon, M. Mawid, B. Sekar, Reduced chemical kinetic mechanisms for JP-8 combustion, 40<sup>th</sup> AIAA Aerospace Sciences Meeting and Exhibit AIAA 2002-0336.
- [20] A. Agosta, N. P. Cernansky, D. L. Miller, T. Faravelli, E. Ranzi, Reference components of jet fuels: kinetic modeling and experimental results, Experimental Thermal and Fluid Science 28 (7) (2004) 701-708.
- [21] G. Freeman, A. H. Lefebvre, Spontaneous ignition characteristics of gaseous hydrocarbon-air mixtures, Combust. Flame 58 (2) (1984) 153-162.
- [22] B. P. Mullins, Autoignition of hydrocarbons, AGARDograph No. 4.
- [23] C. Doute, J.-L. Delfau, R. Akrich, C. Vovelle, Chemical structure of atmospheric pressure premixed *n*-decane and kerosene flames, Combustion Science and Technology 105 (4-6) (1995) 327-344.
- [24] R. O. Foelsche, J. M. Keen, W. C. Solomon, P. L. Buckley, E. Corporan, Nonequilibrium combustion model for fuel-rich gas generators, J. Prop. Power 10 (4) (1994) 461-472.
- [25] J. Emdee, K. Brezinsky, I. Glassman, A kinetic model for the oxidation of toluene near 1200 K, J. Phys. Chem. 96 (5) (1992) 2151-2161.
- [26] C. Vovelle, J.-L. Delfau, M. Reuillon, Formation of aromatic hydrocarbons in decane and kerosene flames at reduced pressure, in: Soot Formation in Combustion, Springer, 1994, pp. 50-65.
- [27] K. M. Leung, Kinetic modeling of hydrocarbon flames using detailed and systematically reduced chemistry, Ph.D. thesis, Mechanical Engineering Dept., Imperial College, University of London (1996).
- [28] L. Q. Maurice, Detailed chemical-kinetic model for aviation fuels, Ph.D. thesis, Mechanical Engineering Dept., Imperial College, University of London (1996).
- [29] R. Lindstedt, L. Maurice, Detailed kinetic modelling of toluene combustion, Comb. Sci. Tech. 120 (1-6) (1996) 119-167.
- [30] W. D. Schulz, Oxidation products of a surrogate jp-8 fuel, ACS Petrol. Chem. Div. Preprints 37 (383-392).
- [31] P. Dagaut, A. El Bakali, A. Ristori, The combustion of kerosene: Experimental results and kinetic modelling using 1-to 3-component surrogate model fuels, Fuel 85 (7) (2006) 944-956.
- [32] M. Braun-Unkloff, P. Frank, A. El Bakali, P. Dagaut, M. Cathonnet, 28th symposium (international) on combustion, Edinburgh 30 (1994) 315.
- [33] E. G. Eddings, S. Yan, W. C. Ciro, A. F. Sarofim, Formulation of a surrogate for the simulation of jet fuel pool fires, Combust. Sci. and Tech. 177 (4) (2005) 715-739.
- [34] S. Humer, A. Frassoldati, S. Granata, T. Faravelli, E. Ranzi, R. Seiser, K. Seshadri, Experimental and kinetic modeling study of combustion of jp-8, its surrogates and reference components in laminar nonpremixed flows, Proceedings of the Combustion Institute 31 (1) (2007) 393 - 400.
- [35] D. Kim, J. Martz, A. Violi, A surrogate for emulating the physical and chemical properties of conventional jet fuel, Combust. Flame 161 (2014) 1489-1498.
- [36] C. Guéret, Ph.D. thesis, Université d'Orléans (1989).
- [37] E. Ranzi, A wide-range kinetic modeling study of oxidation

- and combustion of transportation fuels and surrogate mixtures, *Energy & fuels* 20 (3) (2006) 1024–1032.
- [38] P. Pepiot-Desjardins, Automatic strategies for chemical mechanism reduction, Ph.D. thesis, Stanford University, Department of Mechanical Engineering (June 2008).
- [39] S. Dooley, S. H. Won, M. Chaos, J. Heyne, Y. Ju, F. L. Dryer, K. Kumar, C.-J. Sung, H. Wang, M. A. Oehlschlaeger, R. J. Santoro, T. A. Litzinger, A jet fuel surrogate formulated by real fuel properties, *Combust. Flame* 157 (12) (2010) 2333 – 2339.
- [40] S. Dooley, S. H. Won, J. Heyne, T. I. Farouk, Y. Ju, F. L. Dryer, K. Kumar, X. Hui, C.-J. Sung, H. Wang, M. A. Oehlschlaeger, V. Iyer, S. Iyer, T. A. Litzinger, R. J. Santoro, T. Malewicki, K. Brezinsky, The experimental evaluation of a methodology for surrogate fuel formulation to emulate gas phase combustion kinetic phenomena, *Combust. Flame* 159 (4) (2012) 1444–1466.
- [41] S. Vasu, D. Davidson, R. Hanson, Jet fuel ignition delay times: Shock tube experiments over wide conditions and surrogate model predictions, *Combust. Flame* 152 (2008) 125–143.
- [42] P. Gokulakrishnan, G. Gaines, M. S. Klassen, R. J. Roby, Autoignition of aviation fuels: experimental and modeling study, 43<sup>rd</sup> AIAA/ASME/SAE/ASEE Joint Propulsion Conference & Exhibit AIAA 2007–5701.
- [43] A. J. Dean, O. G. Penyazkov, K. L. Sevruk, B. Varatharajan, Autoignition of surrogate fuels at elevated temperatures and pressures, *Proceedings of the Combustion Institute* 31 (2) (2007) 2481–2488.
- [44] Y. Zhu, S. Li, D. F. Davidson, R. K. Hanson, Ignition delay times of conventional and alternative fuels behind reflected shock waves, *Proc. Combust. Inst.* (in press).
- [45] V. P. Zhukov, V. A. Sechenov, A. Y. Starikovskiy, Autoignition of kerosene (jet-a)/air mixtures behind reflected shock waves, *Fuel* 126.
- [46] D. Valco, C. Allen, E. Toulson, T. Lee, Autoignition behavior of petroleum-based and hydroprocessed renewable jet fuel blends in a rapid compression machine, 51<sup>st</sup> AIAA Aerospace Sciences Meeting including the New Horizons Forum and Aerospace Exposition AIAA 2013–0896.
- [47] R. H. Natelson, M. S. Kurman, N. P. Cernansky, D. L. Miller, Experimental investigation of surrogates for jet and diesel fuels, *Fuel* 87 (2008) 2339–2342.
- [48] C. Ji, Y. Wang, F. Egolfopoulos, Flame studies of conventional and alternative jet fuels, *Journal of Propulsion and Power* 27 (4) (2011) 856.
- [49] X. Hui, K. Kumar, C.-J. Sung, T. Edwards, D. Gardner, Experimental studies on the combustion characteristics of alternative jet fuels, *Fuel* 98 (2012) 176–182.
- [50] D. Singh, T. Nishiie, L. Qiao, Experimental and kinetic modeling study of the combustion of n-decane, jet-a, and s-8 in laminar premixed flames, *Combust. Sci. Tech.* 183 (10) (2011) 1002–1026.
- [51] K. Kumar, C.-J. Sung, X. Hui, Laminar flame speeds and extinction limits of conventional and alternative jet fuels, *Fuel* 90 (3) (2011) 1004–1011.
- [52] T. Malewicki, S. Gudiyaella, K. Brezinsky, Experimental and modeling study on the oxidation of jet a and the n-dodecane/iso-octane/n-propylbenzene/1,3,5-trimethylbenzene surrogate fuel, *Combust. Flame* 160 (2013) 17–30.
- [53] Model fuels consortium, *Reaction Design* (2012).
- [54] G. Blanquart, P. Pepiot-Desjardins, H. Pitsch, Chemical mechanism for high temperature combustion of engine relevant fuels with emphasis on soot precursors, *Combust. Flame* 156 (2009) 588–607.
- [55] K. Narayanaswamy, G. Blanquart, H. Pitsch, A consistent chemical mechanism for the oxidation of substituted aromatic species, *Combust. Flame* 157 (10) (2010) 1879–1898.
- [56] K. Narayanaswamy, P. Pepiot, H. Pitsch, A chemical mechanism for low to high temperature oxidation of *n*-dodecane as a component of transportation fuel surrogates, *Combust. Flame* 161 (4) (2014) 866–884.
- [57] K. Narayanaswamy, H. Pitsch, P. Pepiot, A chemical mechanism for low to high temperature oxidation of methylcyclohexane as a component of transportation fuel surrogates, *Combust. Flame* 162 (4) (2015) 1193–1213.
- [58] D. A. Kouremenos, C. D. Rakopoulos, D. T. Hountalas, Experimental investigation of the performance and exhaust emissions of a swirl chamber diesel engine using JP-8 aviation fuel, *Int. J. Energy Research* 21 (12) (1997) 1173–1185.
- [59] P. Arkoudeas, S. Kalligeros, F. Zannikos, G. Anastopoulos, D. Karonis, D. Korres, E. Lois, Study of using JP-8 aviation fuel and biodiesel in CI engines, *Energy conversion and management* 44 (7) (2003) 1013–1025.
- [60] U.s. department of defense, directive 4140.25 – dod management policy for energy commodities and related services (2004).
- [61] D. M. Korres, D. Karonis, E. Lois, M. B. Linck, A. K. Gupta, Aviation fuel JP-5 and biodiesel on a diesel engine, *Fuel* 87 (1) (2008) 70–78.
- [62] L. Starck, B. Lecoite, L. Forti, N. Jeuland, Impact of fuel characteristics on HCCI combustion: Performances and emissions, *Fuel* 89 (10) (2010) 3069–3077.
- [63] H. J. Curran, P. Gaffuri, W. J. Pitz, C. K. Westbrook, A comprehensive modeling study of *n*-heptane oxidation, *Combust. Flame* 114 (1-2) (1998) 149–177.
- [64] H. J. Curran, P. Gaffuri, W. J. Pitz, C. K. Westbrook, A comprehensive modeling study of iso-octane oxidation, *Combust. Flame* 129 (3) (2002) 253–280.
- [65] S. M. Sarathy, C. K. Westbrook, M. Mehl, W. J. Pitz, C. Togbe, P. Dagaut, H. Wang, M. A. Oehlschlaeger, U. Niemann, K. Seshadri, Comprehensive chemical kinetic modeling of the oxidation of 2-methylalkanes from C<sub>7</sub> to C<sub>20</sub>, *Combust. Flame* 158 (12) (2011) 2338–2357.
- [66] W. J. Pitz, C. V. Naik, T. N. Mhaolduin, C. K. Westbrook, H. J. Curran, J. P. Orme, J. M. Simmie, Modeling and experimental investigation of methylcyclohexane ignition in a rapid compression machine, *Proc. Combust. Inst.* 31 (1) (2007) 267–275.
- [67] P. Pepiot-Desjardins, H. Pitsch, An efficient error propagation based reduction method for large chemical kinetic mechanisms, *Combust. Flame* 154 (2008) 67–81.
- [68] P. Pepiot-Desjardins, H. Pitsch, An automatic chemical lumping method for the reduction of large chemical kinetic mechanisms, *Combust. Theory. Mod.* 12 (6) (2008) 1089–1108.
- [69] [kritikasivaram.github.io](https://github.com/kritikasivaram).
- [70] Reaction design’s model fuel library, [sales@reactiondesign.com](mailto:sales@reactiondesign.com).
- [71] K. Narayanaswamy, P. Pepiot, H. Pitsch, Jet fuels and Fischer-tropsch fuels: Surrogate definition and chemical kinetic modeling, in: U.S National Combustion Meeting, 2013.
- [72] L. Cai, H. Pitsch, Optimized chemical mechanism for combustion of gasoline surrogate fuels, *Combust. Flame*.
- [73] J. Bacha, J. Freel, A. Gibbs, L. Gibbs, G. Hemigaus, N. Hogue, D. Lesnini, J. Lind, J. Maybury, J. Morris, ChevronTexaco Employees and Contractors, Aviation Fuels Technical Review, Technical Report, Chevron Corporation.
- [74] M. Mehl, J.-Y. Chen, W. J. Pitz, S. Sarathy, C. K. Westbrook, An approach for formulating surrogates for gasoline with application toward a reduced surrogate mechanism for cfd engine modeling, *Energy & Fuels* 25 (11) (2011) 5215–5223.
- [75] W. J. Pitz, C. J. Mueller, Recent progress in the development of diesel surrogate fuels, *Progress in Energy and Combustion Science* 37 (3) (2011) 330–350.
- [76] S. Dooley, J. Heyne, S. H. Won, P. Dievart, Y. Ju, F. L. Dryer, Importance of a cycloalkane functionality in the oxidation of a real fuel, *Energy & Fuels* 28 (7649–7661).
- [77] T. Edwards, Liquid fuels and propellants for aerospace propulsion: 1903–2003, *Journal of Propulsion and Power* 19 (6) (2003) 1089–1107.
- [78] J. Bacha, J. Freel, A. Gibbs, L. Gibbs, G. Hemigaus, K. Hoekman, J. Horn, M. Ingham, L. Jossens, D. Kohler, D. Lesnini, J. McGeehan, N. Nikanjam, E. Olsen, R. Organ, B. Scott,

- M. Sztenderowicz, A. Tiedemann, C. Walker, J. Lind, J. Jones, D. Scott, J. Mills, ChevronTexaco Employees and Contractors, Diesel Fuels Technical Review, Technical Report, Chevron Corporation.
- [79] C. V. Naik, K. V. Puduppakkam, A. Modak, E. Meeks, Y. L. Wang, Q. Feng, T. T. Tsotsis, Detailed chemical kinetic mechanism for surrogates of alternative jet fuels, *Combust. Flame* 158 (3) (2011) 434–445.
- [80] Fuel user guide – average survey data, Tech. rep., US Army Tank-Automotive RD&E Center, Fuels and Lubricants Team, Warren, MI (2000).
- [81] J. Edwards, T. Bruno, The properties of s-8, Technical report mipr f4bey6237g001, National Institute of Standards and Technology, Physical and Chemical Properties Division, Boulder, CO (November 2006).
- [82] N. Peters, F. A. Williams, The asymptotic structure of stoichiometric methane-air flames, *Combust. Flame* 68 (2) (1987) 185–207.
- [83] J. Göttgens, F. Mauss, N. Peters, Analytic approximations of burning velocities and flame thicknesses of lean hydrogen, methane, ethylene, ethane, acetylene, and propane flames, in: *Symposium (International) on Combustion*, Vol. 24, Elsevier, 1992, pp. 129–135.
- [84] A. Holley, X. You, E. Dames, H. Wang, F. Egolfopoulos, Sensitivity of propagation and extinction of large hydrocarbon flames to fuel diffusion, *Proceedings of the Combustion Institute* 32 (1) (2009) 1157–1163.
- [85] A. Attili, F. Bisetti, M. E. Mueller, H. Pitsch, Effects of non-unity lewis number of gas-phase species in turbulent non-premixed sooting flames, *Combust. Flame* (submitted).
- [86] K. Narayanaswamy, Chemical kinetic modeling of jet fuel surrogates, Ph.D. thesis, Stanford University, Department of Mechanical Engineering (January 2014).
- [87] H. F. Calcote, D. M. Manos, Effect of molecular structure on incipient soot formation, *Combust. Flame* 49 (1983) 289–304.
- [88] Y. Yang, A. L. Boehman, R. J. Santoro, A study of jet fuel sooting tendency using the threshold sooting index (tsi) model, *Combust. Flame* 149 (1) (2007) 191–205.
- [89] P. Pepiot-Desjardins, H. Pitsch, R. Malhotra, S. R. Kirby, A. L. Boehman, Structural group analysis for soot reduction tendency of oxygenated fuels, *Combust. Flame* 154 (2008) 191–205.
- [90] S. Yan, E. G. Eddings, A. B. Palotas, R. J. Pugmire, A. F. Sarofim, Prediction of sooting tendency for hydrocarbon liquids in diffusion flames, *Energy & Fuels* 19 (6) (2005) 2408–2415.
- [91] S. W. Benson, *Thermochemical Kinetics : Methods for the Estimation of Thermo- chemical Data and Rate Parameters*, Wiley, New York, 1976.
- [92] D. R. Olson, N. T. Meckel, R. Quillian Jr, Combustion characteristics of compression ignition engine fuel components, Tech. rep., SAE Technical Paper (1960).
- [93] M. J. Murphy, J. D. Taylor, R. L. McCormick, Compendium of experimental cetane number data, Tech. rep., National Renewable Energy Laboratory (NREL), Golden, CO. (2004).
- [94] A. Agosta, Development of a chemical surrogate for jp-8 aviation fuel using a pressurized flow reactor, Master’s thesis, Drexel University (2002).
- [95] P. Ghosh, S. B. Jaffe, Detailed composition-based model for predicting the cetane number of diesel fuels, *Industrial & engineering chemistry research* 45 (1) (2006) 346–351.
- [96] I. P. Androulakis, M. D. Weisel, C. S. Hsu, K. Qian, L. A. Green, J. T. Farrell, K. Nakakita, An integrated approach for creating model diesel fuels, *Energy & fuels* 19 (1) (2005) 111–119.
- [97] C. V. Naik, K. Puduppakkam, C. Wang, J. Kottalam, L. Liang, D. Hodgson, E. Meeks, Applying detailed kinetics to realistic engine simulation: The surrogate blend optimizer and mechanism reduction strategies, Tech. rep., SAE Technical Paper (2010).
- [98] M. Huber, E. Lemmon, T. Bruno, Surrogate mixture models for the thermophysical properties of aviation fuel jet-a, *Energy & Fuels* 24 (6) (2010) 3565–3571.
- [99] K. Anand, Y. Ra, R. Reitz, B. Bunting, Surrogate model development for fuels for advanced combustion engines, *Energy & Fuels* 25 (4) (2011) 1474–1484.
- [100] C. J. Mueller, W. J. Cannella, T. J. Bruno, B. Bunting, H. D. Dettman, J. A. Franz, M. L. Huber, M. Natarajan, W. J. Pitz, M. A. Ratcliff, K. Wright, Methodology for formulating diesel surrogate fuels with accurate compositional, ignition-quality, and volatility characteristics, *Energy & Fuels* 26 (6) (2012) 3284–3303.
- [101] MATLAB, version 7.10.0 (R2010a), The MathWorks Inc., Natick, Massachusetts, 2010.
- [102] A. Ahmed, G. Goteng, V. S. Shankar, K. Al-Qurashi, W. L. Roberts, S. M. Sarathy, A computational methodology for formulating gasoline surrogate fuels with accurate physical and chemical kinetic properties, *Fuel* 143 (2015) 290–300.
- [103] A. Roubaud, R. Minetti, L. Sochet, Oxidation and combustion of low alkylbenzenes at high pressure: Comparative reactivity and auto-ignition, *Combust. Flame* 121 (2000) 535–541.
- [104] D. B. Lenhart, D. L. Miller, N. P. Cernansky, The oxidation of jp-8, jet-a, and their surrogates in the low and intermediate temperature regime at elevated pressures, *Combustion science and technology* 179 (5) (2007) 845–861.
- [105] H. Pitsch, M. Bollig, Flamemaster, a computer code for homogeneous and one-dimensional laminar flame calculations, Institut für Technische Mechanik, RWTH Aachen.
- [106] D. C. Horning, D. F. Davidson, R. K. Hanson, Study of the high temperature autoignition of *n*-alkane/O<sub>2</sub>/Ar mixtures, *J. Prop. Power* 18 (2) (2002) 363–371.
- [107] S. Honnet, K. Seshadri, U. Niemann, N. Peters, A surrogate fuel for kerosene, *Proceedings of the Combustion Institute* 32 (1) (2009) 485 – 492.
- [108] T. Malewicki, K. Brezinsky, Experimental and modeling study on the pyrolysis and oxidation of *n*-decane and *n*-dodecane, *Proc. Combust. Inst.* 34 (1) (2013) 361–368.
- [109] T. Malewicki, A. Comandini, K. Brezinsky, Experimental and modeling study on the pyrolysis and oxidation of iso-octane, *Proc. Combust. Inst.* 34 (2013) 353–360.
- [110] S. Gudiyella, K. Brezinsky, High pressure study of *n*-propylbenzene oxidation, *Combust. Flame* 159 (3) (2012) 940–958.
- [111] J. Bugler, K. P. Somers, E. J. Silke, H. J. Curran, Revisiting the kinetics and thermodynamics of the low-temperature oxidation pathways of alkanes: A case study of the three pentane isomers, *The Journal of Physical Chemistry A*.
- [112] L. Cai, H. Pitsch, S. M. Sarathy, V. Raman, J. Bugler, H. Curran, Optimized rate rules for model development of normal alkanes, *Combust. Flame* (submitted).
- [113] C. Ji, F. N. Egolfopoulos, Flame propagation of mixtures of air with binary liquid fuel mixtures, *Proceedings of the Combustion Institute* 33 (1) (2011) 955–961.
- [114] T. Hirasawa, C. J. Sung, A. Joshi, Z. Yang, H. Wang, C.K.Law, Determination of laminar flame speeds using digital particle image velocimetry: Binary fuel blends of ethylene, *n*-butane and toluene, *Proc. Combust. Inst.* 29 (2002) 1427–1434.